



## Design, synthesis, *in vitro* and *in vivo* biological evaluation of pyranone-piperazine analogs as potent antileishmanial agents



Shachi Mishra<sup>a,1</sup>, Naveen Parmar<sup>b,c,1</sup>, Pragya Chandrakar<sup>b,c</sup>, Chandra Prakash Sharma<sup>a</sup>, Sajiya Parveen<sup>c,a</sup>, Ravi P. Vats<sup>c,a</sup>, Anuradha Seth<sup>b,c</sup>, Atul Goel<sup>c,a,\*\*</sup>, Susanta Kar<sup>b,c,\*</sup>

<sup>a</sup> Medicinal and Process Chemistry Division, CSIR-Central Drug Research Institute, BS-10/1, Sector 10, Jankipuram Extension, Sitapur Road, Lucknow, 226031, India

<sup>b</sup> Molecular Parasitology & Immunology Division, CSIR-Central Drug Research Institute, BS-10/1, Sector 10, Jankipuram Extension, Sitapur Road, Lucknow, 226031, India

<sup>c</sup> Academy of Scientific and Innovative Research (AcSIR), Sector 19, Kamla Nehru Nagar, Ghaziabad, Uttar Pradesh, 201 002, India

### ARTICLE INFO

#### Article history:

Received 17 July 2020

Received in revised form

23 April 2021

Accepted 24 April 2021

Available online 4 May 2021

#### Keywords:

Visceral leishmaniasis (VL)

2-Pyranone

Phenylpiperazine substituted pyranones

Antileishmanial activity

Mitochondrial dysfunction

Apoptosis

### ABSTRACT

The current therapeutic regimen for visceral leishmaniasis is inadequate and unsatisfactory due to toxic side effects, high cost and emergence of drug resistance. Alternative, safe and affordable antileishmanials are, therefore, urgently needed and toward these we synthesized a series of arylpiperazine substituted pyranone derivatives and screened them against both *in vitro* and *in vivo* model of visceral leishmaniasis. Among 22 synthesized compounds, **5a** and **5g** showed better activity against intracellular amastigotes with an IC<sub>50</sub> of 11.07 μM and 15.3 μM, respectively. In the *in vivo*, **5a** significantly reduced hepatic and splenic amastigotes burden in Balb/c mice model of visceral leishmaniasis. On a mechanistic node, we observed that **5a** induced direct *Leishmania* killing via mitochondrial dysfunction like cytochrome *c* release and loss of membrane potential. Taken together, our results suggest that **5a** is a promising lead for further development of antileishmanial drugs.

© 2021 Elsevier Masson SAS. All rights reserved.

### 1. Introduction

Leishmaniasis is a disease caused by obligate intra-macrophage protozoan parasite that belongs to the genus, *Leishmania*. Visceral leishmaniasis (VL) also known as kala azar is mainly caused by *Leishmania donovani* in Indian subcontinent and East Africa, and *Leishmania infantum* in Europe and Latin America [1]. VL is a lethal form of leishmaniasis, and is responsible for high mortality and morbidity rate if left untreated. Since there is no effective vaccines

candidate, chemotherapeutic regimen remains a basis for the treatment of VL. Pentavalent antimonials (Pentostam and Glucantime) were used as a first line treatment for VL for more than half a century [2], however, rates of resistance have been well documented and reported to be higher than 60% in parts of the state of Bihar, in north-east India. In addition, therapeutic options for VL have been improved by using of oral drug miltefosine, a variety of liposomal formulations of amphotericin B, aminoglycoside antibiotic paromomycin and pentamidine [3]. However,

**Abbreviations:** CC<sub>50</sub>, 50% reduction of viability of treated cells with respect to untreated cells; DMSO, dimethyl sulfoxide; FACS, Fluorescence-Activated Cell Sorting; FBS, fetal bovine serum; HPLC, high-performance liquid chromatography; HRMS, high-resolution mass spectrometry; IC<sub>50</sub>, half-maximal inhibitory concentration; ip, intraperitoneal; IR, infrared spectroscopy; LDU, *Leishmania donovani* unit; MTT, 3-(4,5-dimethylthiazol-2-yl)-2,5-diphenyltetrazolium bromide; SI, selectivity index; MMP, mitochondrial membrane potential; PI, propidium iodide; TUNEL, terminal deoxynucleotidyl transferase dUTP nick end labeling; NMR, nuclear magnetic resonance; TLC, thin-layer chromatography; VL, visceral leishmaniasis.

\* Corresponding author. Molecular Parasitology & Immunology Division, CSIR-Central Drug Research Institute, BS-10/1, Sector 10, Jankipuram Extension, Sitapur Road, Lucknow, 226031, India.

\*\* Corresponding author. Medicinal and Process Chemistry Division, CSIR-Central Drug Research Institute, BS-10/1, Sector 10, Jankipuram Extension, Sitapur Road, Lucknow, 226031, India.

E-mail addresses: [atul\\_goel@cdri.res.in](mailto:atul_goel@cdri.res.in) (A. Goel), [susantakar@cdri.res.in](mailto:susantakar@cdri.res.in) (S. Kar).

<sup>1</sup> S.M. and N.P. contributed equally to this work.

concerns like teratogenicity, gastrointestinal side effects, high cost, long elimination half life and parenteral administration for longer duration are associated with these chemotherapeutic agents [4]. These issues emphasize an urgent need of antileishmanial drug discovery programme to identify novel, safer and cheaper chemotherapeutic regimen against leishmaniasis. *L. donovani* has the capacity to successfully survive within hostile environment and avoiding host immune defense mechanisms by intracellular growth [5]. Therefore, the introduction of novel synthetic compounds with improved pharmacological properties and effective killing of intracellular forms of *Leishmania* parasite is essential for the treatment of any form of leishmaniasis. 2-Pyranone belongs to privileged class of heterocyclic scaffold and due to its pharmacophoric properties, has attracted much attention. Most of the compounds display strong biological activities such as cytotoxic, antibiotic, antihyperglycemic and antifungal activities [6–9]. Some pyranones and their isosteres have also been found to exhibit promising antileishmanial activity (Fig. 1) [10,11]. Further, piperazines are also an important heterocyclic scaffold and several diarylpiperazine analogs possess good antileishmanial activity (Fig. 1) [12–16]. Therefore, in our endeavor to find new antileishmanials with better efficacy and less toxicity, we designed, synthesized and screened a series of arylpiperazine substituted pyranone derivatives against both *in vitro* and *in vivo* experimental model of VL. To further extend the SAR, ring transformation of pyranone core was done with dihydrothiophen-3(2H)-one and tetrahydro-4H-thiopyran-4-one.

## 2. Results and discussion

### 2.1. Chemistry

A series of 2H-pyranones appended with arylpiperazine was synthesized as depicted in Scheme 1. The precursors 2H-pyranones derivatives **3a–j** were prepared from ketene-S,S-acetal (**1**) and substituted cyclic or acyclic methylene carbonyl compounds **2a–j** through carbanion-induced ring formation reaction [17]. Further for the synthesis of our designed piperazinyl-pyranone hybrid molecule, the methylsulfonyl group of **3a–j** was replaced with arylpiperazine **4a** by refluxing in methanol for 1–4 h to furnish **5a–j** in good yields. In order to establish structure-activity relationships, different electron withdrawing and electron releasing groups were incorporated onto the arylpiperazine substrates **4b–d** to furnish pyranone-piperazine derivatives **5k–q**. Further, Michael addition of

the conjugate base of **6a,b** at the electrophilic C-6 position of substituted 2H-pyran-2-ones **5a,c,g,i** gave the respective ring transformed products **7a–e** in good yields (Scheme 2).

#### 2.1.1. *In silico* prediction of physicochemical properties of 5a–q and 7a–e

*In silico* predictions of physicochemical properties, pharmacokinetics and toxicity profiling provide useful insight for drugability of newly synthesized derivatives. The molecular descriptors such as TPSA, log P, nRotB, and molecular weight, number of hydrogen bond donors and acceptors of Lipinski's rule were calculated for all the synthesized compounds using Molinspiration software [18]. Lipinski's rule of five (RO5) states that most "drug like" molecules have  $\log P \leq 5$ , molecular weight  $\leq 500$ , number of hydrogen bond acceptors  $< 10$ , and number of hydrogen bond donors  $\leq 5$  [19]. The expansion of these rules evolved the nRot bond and PSA descriptors in which it is desirable that there are 10 or fewer rotatable bonds and a polar surface area equal to or less than  $140 \text{ \AA}^2$  for excellent oral absorption of a drug candidate [20,21]. TPSA is the surface areas that are occupied by oxygen and nitrogen atoms and by hydrogen atoms linked to them. Therefore, it is closely related to the hydrogen bonding potential of a compound. MiLogP (octanol/water partition coefficient) is calculated by the methodology developed by Molinspiration as a sum of fragment based contributions and correction factors [18]. *In silico* study revealed that all the synthesized compounds (**5a–q** and **7a–e**) have TPSA values  $< 140 \text{ \AA}^2$ , nRotB = 2 to 4, hydrogen bond acceptors = 4 to 7, hydrogen bond donor = 0 to 1, and molecular volume 334 to 432 ( $\text{\AA}^3$ ) thus, they are foreseen to display good oral absorption. For a molecule being well absorbed, miLogP value must be in the range of -0.4 to +5. Our results indicated that, pyranone-piperazine series **5a–q** (except **5l** and **5m**) was found to have miLogP values within the acceptable range and thus they were predicted to have good oral absorption (Table 1). While in series of 1,3-dihydrobenzo[*c*]thiophene-4-carbonitrile (**7a–c**) and 8-(aryl/heteroaryl)isothiochromane-5-carbonitrile (**7d, e**), it is noteworthy that all analyzed compounds have one or two violations of Lipinski's rule (logP and molecular weight, Table 1) except **7b**.

#### 2.1.2. Theoretical toxicity profiling of synthesized compounds 5a–q and 7a–e

In order to evaluate the fragment-based toxicity risks (mutagenic, tumorigenic and irritant effects) of the synthesized derivatives and also for comparison with standard drug Miltefosine,

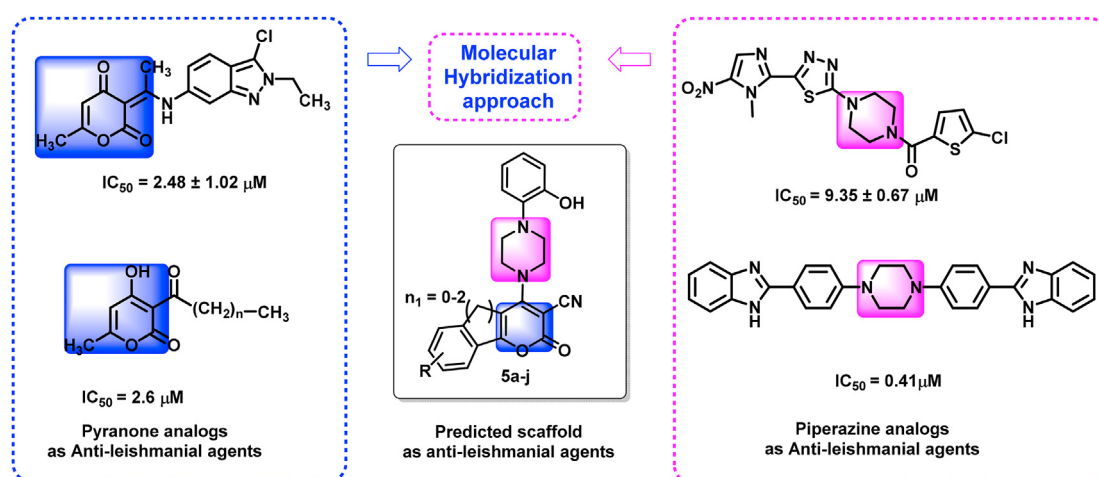
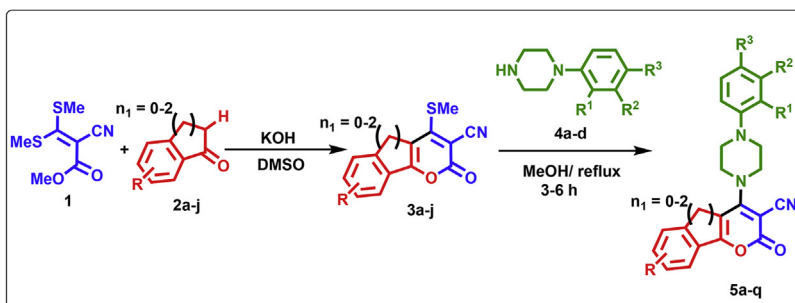
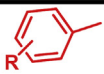
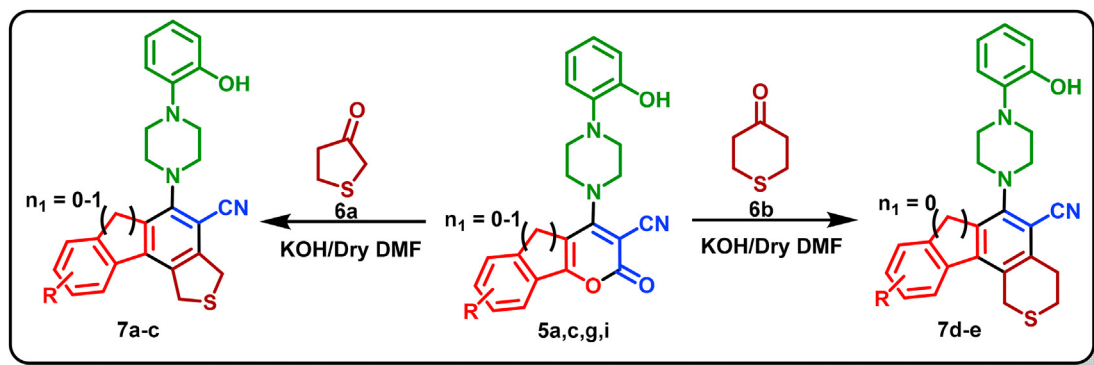


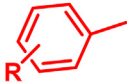
Fig. 1. Strategy for designing pyranone and piperazine (molecular hybrid approach) analogs as Anti-leishmanial agents.



entry		$n_1$	$R^1$	$R^2$	$R^3$	Yield(%)
5a	C <sub>6</sub> H <sub>5</sub>	0	OH	H	H	72
5b	4-Cl-C <sub>6</sub> H <sub>4</sub>	0	OH	H	H	68
5c	4-Br-C <sub>6</sub> H <sub>4</sub>	0	OH	H	H	66
5d	4-Me-C <sub>6</sub> H <sub>4</sub>	0	OH	H	H	62
5e	4-MeO-C <sub>6</sub> H <sub>4</sub>	0	OH	H	H	61
5f	1-naphthyl	0	OH	H	H	58
5g	thienyl	0	OH	H	H	55
5h	5-Br-thienyl	0	OH	H	H	50
5i	C <sub>6</sub> H <sub>4</sub>	1	OH	H	H	47
5j	C <sub>6</sub> H <sub>4</sub>	2	OH	H	H	44
5k	C <sub>6</sub> H <sub>5</sub>	0	Cl	H	H	65
5l	4-Cl-C <sub>6</sub> H <sub>4</sub>	0	Cl	H	H	66
5m	4-Br-C <sub>6</sub> H <sub>4</sub>	0	Cl	H	H	62
5n	4-MeO-C <sub>6</sub> H <sub>4</sub>	0	Cl	H	H	60
5o	C <sub>6</sub> H <sub>5</sub>	0	H	Cl	H	52
5p	C <sub>6</sub> H <sub>5</sub>	0	OMe	H	H	68
5q	4-Br-C <sub>6</sub> H <sub>4</sub>	0	OMe	H	H	64

**Scheme 1.** Synthesis of 4-(4-(2-hydroxyphenyl)piperazin-1-yl)-2-oxo-6-(aryl/heteroaryl)-2H-pyran-3-carbonitrile (**5a-q**).



entry		$n_1$	Yield (%)
7a	C <sub>6</sub> H <sub>5</sub>	0	55
7b	thienyl	0	50
7c	C <sub>6</sub> H <sub>5</sub>	1	45
7d	thienyl	0	48
7e	4-Br-C <sub>6</sub> H <sub>4</sub>	0	52

**Scheme 2.** Synthesis of 5-(4-(2-hydroxyphenyl)piperazin-1-yl)-7-(aryl/hetero-aryl)-1,3-dihydrobenzo[*c*]thiophene-4-carbonitrile (**7a-c**) and 6-(4-(2-hydroxy-phenyl)piperazin-1-yl)-8-(aryl/heteroaryl)isothiochromane-5-carbonitrile (**7d,e**).

the online web free software OSIRIS property explorer [22] was used. This software comprehends the database of known drugs and nondrug-like Fluka compounds to assess the frequency of each fragment in the single molecule. All results using OSIRIS software are shown in Table 2. The theoretical toxicity analysis (tumorigenic, mutagenic profiles) of the synthesized compounds revealed that most of the compounds showed no risk of being mutagenic and tumorigenic effect, like the antileishmanial drug Miltefosine, while two compounds namely **5f** and **7c** showed some risk of mutagenic and tumorigenic effect. All the synthesized compounds were predicted to have some irritant effect (Table 2). Overall, based on the *in silico* studies, it was observed that a series of **5a-q** showed good drug-likeness as compared to the compounds **7a-e**.

## 2.2. *In vitro* anti-leishmanial activity against extracellular promastigotes and intracellular amastigotes

To check the anti-leishmanial potential, we screened the synthesized pyranone-piperazine derivatives of **5a-q** and **7a-e** against both extracellular and intracellular stages of *Leishmania* parasites.

Initially all the synthesized derivatives were evaluated at 25  $\mu$ M and 50  $\mu$ M concentration against both life stages of the parasite taking miltefosine as a reference drug. The anti-leishmanial activity of all the synthesized compounds is represented in Table 3. We observed that two compounds **5a** and **5g** showed more than 80% inhibition of intracellular amastigotes and extracellular promastigotes at both concentrations (Table 3). In order to establish structure-activity relationships (SARs), different electron donating and withdrawing substituents at C4 and C6 positions of pyranones **5a-q** were incorporated. So the *in vitro* antileishmanial activity profile of the compounds **5a-e** revealed that the substitution of electron withdrawing groups (EWG) such as chloro (**5b**) and bromo (**5c**) to the benzene ring led to marked reduction in both anti-promastigote and anti-amastigote activity. Again, substitution of electron donating groups such as methyl (**5d**) or methoxy (**5e**) at the same position (C6) also displayed less parasitic inhibition than the unsubstituted phenyl moiety (**5a**). Replacing the phenyl ring with more bulkier substituent like 1-naphthyl moiety (**5f**) resulted in significant inhibition (78.6 and 80.8%) at 50  $\mu$ M concentration against both promastigote and amastigote respectively but the

**Table 1**  
Molecular properties calculated by Molinspiration.

Entry	M.W	LogP	HBA	HBD	TPSA(Å <sup>2</sup> )	nRotB	Lipinski's Violation	Molecular Volume (Å <sup>3</sup> )
5a	373.41	3.66	6	1	80.71	3	0	334.22
5b	407.86	4.34	6	1	80.71	3	0	347.76
5c	452.31	4.47	6	1	80.71	3	0	352.11
5d	387.44	4.11	6	1	80.71	3	0	350.78
5e	403.44	3.72	7	1	89.94	4	0	359.77
5f	423.47	4.82	6	1	80.71	3	0	378.21
5g	<b>379.44</b>	<b>3.44</b>	<b>6</b>	<b>1</b>	<b>80.71</b>	<b>3</b>	<b>0</b>	<b>324.93</b>
5h	458.34	4.38	6	1	80.71	3	0	342.82
5i	385.42	3.74	6	1	80.71	2	0	340.18
5j	399.45	3.76	6	1	80.71	2	0	356.98
5k	391.86	4.56	5	0	60.48	3	0	339.74
5l	426.30	5.24	5	0	60.48	3	1	353.28
5m	470.75	5.37	5	0	60.48	3	1	357.63
5n	421.88	4.61	6	0	69.71	4	0	365.29
5o	391.86	4.58	5	0	60.48	3	0	339.74
5p	393.47	3.72	6	0	69.71	4	0	342.46
5q	466.33	4.75	6	0	69.71	4	0	369.64
7a	413.55	5.02	4	1	50.50	3	1	374.56
7b	419.57	4.18	4	1	50.50	3	0	365.27
7c	425.56	5.10	4	1	50.50	2	1	380.52
7d	433.60	5.01	4	1	50.50	3	1	382.07
7e	<b>506.47</b>	6.04	4	1	50.50	3	2	409.25
Miltefosine	407.58	-0.21	5	0	58.60	20	0	432.32

M.W.: molecular weight; LogP: logarithm of n-octanol-water partition coefficient; HBA (nON): number of hydrogen bond acceptors or no of oxygen and nitrogen atom; HBD (nOHNH): number of hydrogen bond donors or number of NH, OH bond; TPSA: topological polar surface area; nRotB: number of rotatable bonds.

**Table 2**  
Theoretical toxicity evaluation of synthesized compounds 5a-q and 7a-e.

Entry	Mutagenic	Tumorigenic	Irritant	Entry	Mutagenic	Tumorigenic	Irritant
5a	(-)	(-)	(++)	5l	(-)	(-)	(++)
5b	(-)	(-)	(++)	5m	(-)	(-)	(++)
5c	(-)	(-)	(++)	5n	(-)	(-)	(++)
5d	(-)	(-)	(++)	5o	(-)	(-)	(++)
5e	(-)	(-)	(++)	5p	(-)	(-)	(++)
5f	(+)	(++)	(++)	5q	(-)	(-)	(++)
5g	(-)	(-)	(++)	7a	(-)	(-)	(-)
5h	(-)	(-)	(++)	7b	(-)	(-)	(-)
5i	(-)	(-)	(++)	7c	(++)	(++)	(-)
5j	(-)	(-)	(++)	7d	(-)	(-)	(-)
5k	(-)	(-)	(++)	7e	(-)	(-)	(-)
Miltefosine	(-)	(-)	(-)				

The scale of toxicity risk ranges from none (-), low (+), high (++) calculated by using OSIRIS Property Explorer.

activity was lesser than 5a. Interestingly, when phenyl moiety was replaced with thienyl ring (5g) at C6 position of pyranone framework, the remarkable inhibitory activity was observed ( $\approx 90\%$ ) at 50  $\mu\text{M}$  concentration against both life stages of the parasite (Table 3). Further, by blocking the rotational freedom of phenyl ring at C5–C6 positions of the pyranone ring to form indeno[1,2-b]pyran-2(5H)-one (5i) and 5,6-dihydro-2H-benzo[h]chromen-2-one (5j) compounds resulted in lesser antileishmanial activity as compared to 5a.

Further in order to examine SAR at C4 position of pyranone ring, different phenyl piperazine derivatives linked with electron withdrawing and releasing groups (EWG and ERG) were employed to prepare compounds (5k–q) and further subjected to *in vitro* antileishmanial activity evaluation (Table 3). When hydroxy group of phenylpiperazine in 5a was replaced by electron withdrawing chloro group (5k), it displayed moderate anti-leishmanial activity whereas when hydroxy group of phenylpiperazine in 5g was replaced by an electron donating methoxy group (5p), the antileishmanial activity was significantly decreased possibly due to inhibition of hydrogen bonding with the receptor.

The synthesized dihydrothiophen-3(2H)-one (7a–c) and tetrahydro-4H-thiopyran-4-one (7d–e) showed either no inhibition or

weak to moderate activity, implying that pyranone ring play an important role is displaying anti-leishmanial activity. The *in vitro* activity profile of 5a–q and 7a–e was well in agreement with the *in silico* analysis of the compounds.

Overall, on the basis of *in silico* (physicochemical) and *in vitro* studies, it was found that compounds 5a and 5g exhibited antileishmanial efficacy superior to other derivatives. So compounds 5a and 5g were selected for further *in vivo* studies.

The efficacy of 5a and 5g on the inhibition of promastigote and amastigote multiplication was then checked in a time-dependent fashion by MTT assay and luciferase assay respectively. A time-dependent killing of promastigotes and amastigotes were observed treated with 5a and 5g with maximum inhibition observed at 72 h post-treatment for both the compounds (Fig. 2A and B). Similarly, dose response analysis revealed dose dependent inhibition of amastigotes up to 50  $\mu\text{M}$  with a maximum killing of  $>89\%$  by both 5a and 5g which was remained same up to 100  $\mu\text{M}$  (Fig. 2C) as determined by luciferase assay. The IC<sub>50</sub> was found to be  $11.07 \pm 1.15 \mu\text{M}$  and  $15.3 \pm 2.1 \mu\text{M}$  for 5a and 5g respectively against intracellular amastigotes at 72 h post treatment, as compared to IC<sub>50</sub> of reference drug, miltefosine, which was reported to be  $12.77 \pm 0.47 \mu\text{M}$ . Since compounds 5d, 5e, 5f, and 5h showed

**Table 3**  
*In vitro* anti-leishmanial activity of 5a-q and 7a-e.

Compound code	Antipromastigote activity		Antiamastigote activity	
	25 $\mu$ M	50 $\mu$ M	25 $\mu$ M	50 $\mu$ M
<b>5a</b>	82.7 $\pm$ 9.4	85.2 $\pm$ 8.2	84.2 $\pm$ 6.3	95.7 $\pm$ 3.2
5b	NI	25.01 $\pm$ 3.1	NI	NI
5c	NI	NI	14.49 $\pm$ 1.5	35.07 $\pm$ 2.9
5d	54.7 $\pm$ 6.2	72.8 $\pm$ 6.9	77.3 $\pm$ 4.9	83.2 $\pm$ 5.2
5e	78.3 $\pm$ 8.4	86.3 $\pm$ 7.4	51.8 $\pm$ 4.9	84.4 $\pm$ 5.3
5f	77.3 $\pm$ 5.7	78.6 $\pm$ 6.4	71.4 $\pm$ 6.3	80.8 $\pm$ 5.4
<b>5g</b>	81.3 $\pm$ 9.5	90.2 $\pm$ 7.2	84.7 $\pm$ 5.6	89.3 $\pm$ 6.2
5h	52.1 $\pm$ 4.3	88.1 $\pm$ 7.2	74.8 $\pm$ 5.2	85.07 $\pm$ 6.8
5i	14.2 $\pm$ 2.4	82.2 $\pm$ 6.3	37.8 $\pm$ 2.6	60.03 $\pm$ 4.8
5j	35.9 $\pm$ 3.9	81.3 $\pm$ 7.4	37.8 $\pm$ 4.8	64.8 $\pm$ 4.1
5k	46.88 $\pm$ 3.05	72.91 $\pm$ 1.49	49.24 $\pm$ 3.31	73.65 $\pm$ 1.9
5l	55.21 $\pm$ 3.15	58.30 $\pm$ 1.09	73.10 $\pm$ 3.13	71.02 $\pm$ 1.2
5 m	57.92 $\pm$ 3.19	66.46 $\pm$ 3.28	60.5 $\pm$ 3.57	68.51 $\pm$ 2.71
5n	60.32 $\pm$ 0.89	69.21 $\pm$ 1.64	50.96 $\pm$ 3.4	62.45 $\pm$ 1.56
5o	44.01 $\pm$ 2.94	57.31 $\pm$ 2.89	47.44 $\pm$ 3.87	72.13 $\pm$ 3.74
5p	48.11 $\pm$ 2.27	62.24 $\pm$ 3.77	52.18 $\pm$ 5.47	71.19 $\pm$ 2.7
5q	56.63 $\pm$ 0.75	61.17 $\pm$ 1.99	43.31 $\pm$ 4.53	58.34 $\pm$ 2.76
7a	82.1 $\pm$ 6.3	87.8 $\pm$ 6.9	NI	NI
7b	NI	4.8 $\pm$ 2.6	60.1 $\pm$ 4.9	79.3 $\pm$ 5.2
7c	NI	NI	45.5 $\pm$ 3.9	57.3 $\pm$ 4.7
7d	NI	NI	65.02 $\pm$ 5.3	72.6 $\pm$ 3.9
7e	NI	33.3 $\pm$ 4.1	71.02 $\pm$ 6.3	83.3 $\pm$ 5.7
<b>Miltefosine</b>	99.4 $\pm$ 0.4	99.7 $\pm$ 0.2	91.2 $\pm$ 0.7	95.3 $\pm$ 0.6

Percent inhibition is expressed as mean  $\pm$  standard deviation of at least three independent experiments done in replicate for each compound. NI—No Inhibition.

significant antileishmanial activity (>80% inhibition) against intracellular amastigote form at 50  $\mu$ M, we proceeded to check their effect in a dose-dependent manner (3.125–50  $\mu$ M). The observed IC<sub>50</sub> of all four compounds against intracellular amastigotes followed a range between 13 and 24  $\mu$ M, which was higher than **5a** (Fig. 2E). However, in terms of maximum inhibition of intracellular parasite growth, compounds **5a** and **5g** showed most superior efficacy (~90% killing of amastigotes), hence we proceeded with these two compounds for further safety index determination.

The cytotoxicity assay was performed next to differentiate between actual inhibitory activity against amastigotes or cytotoxicity against macrophages and we found that both these compounds were non toxic for macrophages even at higher concentration with CC<sub>50</sub> of 350.8  $\mu$ M and 310.9  $\mu$ M for **5a** and **5g**, respectively (Fig. 2D). Altogether, these results prompted us to evaluate the anti-leishmanial effect of both these derivatives in *in vivo* model of VL of *L. donovani*.

### 2.3. Evaluation of anti-leishmanial potential against Balb/c mice model of VL

The *in vitro* active compounds with a good safety profile (**5a** and **5g**) were further selected for *in vivo* screening which was conducted in Balb/c mice (acute model) infected with *L. donovani*. For these, 15 days infected Balb/c mice were administered intraperitoneally with **5a** and **5g** for five consecutive days at a dose of 50 mg/kg. Animals were sacrificed 1 wk post treatment to assess organ parasite burden. Compound **5a** showed better antileishmanial efficacy than **5g** as we observed a significant reduction of intracellular amastigotes in liver and spleen tissue of Balb/c mice after 1 wk post treatment. The reduction in amastigotes multiplication in the liver and spleen of *L. donovani*-infected Balb/c mice treated with **5a** were found to be 67.3%, and 56.9%, respectively (Fig. 3A and B). Miltefosine was used as standard reference drug showed >97% inhibition of organ parasite burden in infected Balb/c mice, when given at a dose of 25 mg/kg/day for 5 days (data not shown). Since cytokines play an important role in the progression or resolution of

visceral leishmaniasis, therefore in this context, we measured the level of host protective proinflammatory cytokines and anti-inflammatory cytokines. However, we did not find increased level of host defensive IFN- $\gamma$  (Fig. 3C) and IL-12 (Fig. 3D), in culture supernatant isolated from splenocytes of **5a** treated mice infected with *L. donovani*. Similarly, expression of disease progressive IL-10 (Fig. 3E) and TGF- $\beta$  (Fig. 3F) were also not downregulated in splenocytes of **5a** treated mice infected with *L. donovani*. On the contrary, standard anti-leishmanial drug Miltefosine markedly increase host defensive IFN- $\gamma$  and IL-12 (Fig. 3C and D) along with significant attenuation of IL-10 and TGF- $\beta$  (Fig. 3E and F). These observations allowed us to speculate for the direct killing of *L. donovani* parasite by compound **5a** as it did not possess any immunomodulatory properties.

### 2.4. 5a induces mitochondrial apoptosis in extracellular promastigotes

To examine whether *L. donovani* promastigotes undergo apoptosis which is a well known mode of direct killing of parasite, untreated and **5a** treated promastigotes were stained with annexin V and propidium iodide. As shown in Fig. 4A, flow cytometric analysis revealed that **5a** exposure for different time periods at maximum inhibitory concentration (50  $\mu$ M) resulted in increased populations of apoptotic cells (16.6% at 24 h, 41.4% at 48 h and 54.5% at 72 h post treatment) as compared to vehicle treated promastigotes (Fig. 4A). Depolarization of mitochondrial membrane potential (MMP) is one of the characteristic features of mitochondrial dysfunction mediated apoptosis. Therefore, to investigate whether **5a** treatment (both IC<sub>50</sub> and 50  $\mu$ M concentration) in promastigotes is associated with mitochondrial dysfunction, we analyzed MMP changes in treated promastigotes by staining with JC-1 dye which at a lower potential forms monomers and emits green fluorescence in the cytoplasm. Flow cytometric analysis also revealed a time dependent loss in MMP (as evident by increase in green fluorescence) in **5a** treated promastigotes which was maximum at 72 h post treatment (Fig. 4B). The loss in MMP was drastically reduced (22.9%) when the parasite was treated with IC<sub>50</sub> of **5a** (Fig. 4C). The maximum fluorescence signal shifted from red to green was observed in CCCP-treated parasites (a mitochondrial uncoupler, used as a positive control), which suggested JC-1 sensitivity toward membrane potential in leishmanial cells. Cytochrome c release from the dysfunctional mitochondria to cytosol is an important event in apoptosis [23] and therefore we next examined whether the translocation of cytochrome c from mitochondria to cytosol is initiated by **5a** treatment in promastigotes or not. We observed very little abundance of cytochrome c in the cytosolic fractions of control promastigotes thereby suggesting intact mitochondria. However, cytosolic abundance of cytochrome c in **5a** treated promastigotes gradually increased, starting at 12 h and being maximum between 48 h and 72 h, along with its gradual disappearance from mitochondria, as observed by immunoblotting (Fig. 4D). To further confirm the induction of apoptosis in **5a** treated promastigotes, we detected DNA fragmentation as a marker of apoptosis by terminal deoxynucleotidyl transferase dUTP nick end labeling (TUNEL) staining. As shown in Fig. 4D, the promastigotes treated with **5a** showed significant TUNEL positivity as evident by bright green fluorescence in the nucleus because of DNA fragmentation, which was not detected in non-treated and vehicle (0.1% DMSO) treated promastigotes (Fig. 4E).

## 3. Conclusion

A novel series of arylpiperazine containing pyranones and benzene cored arylpiperazine was prepared. All synthesized

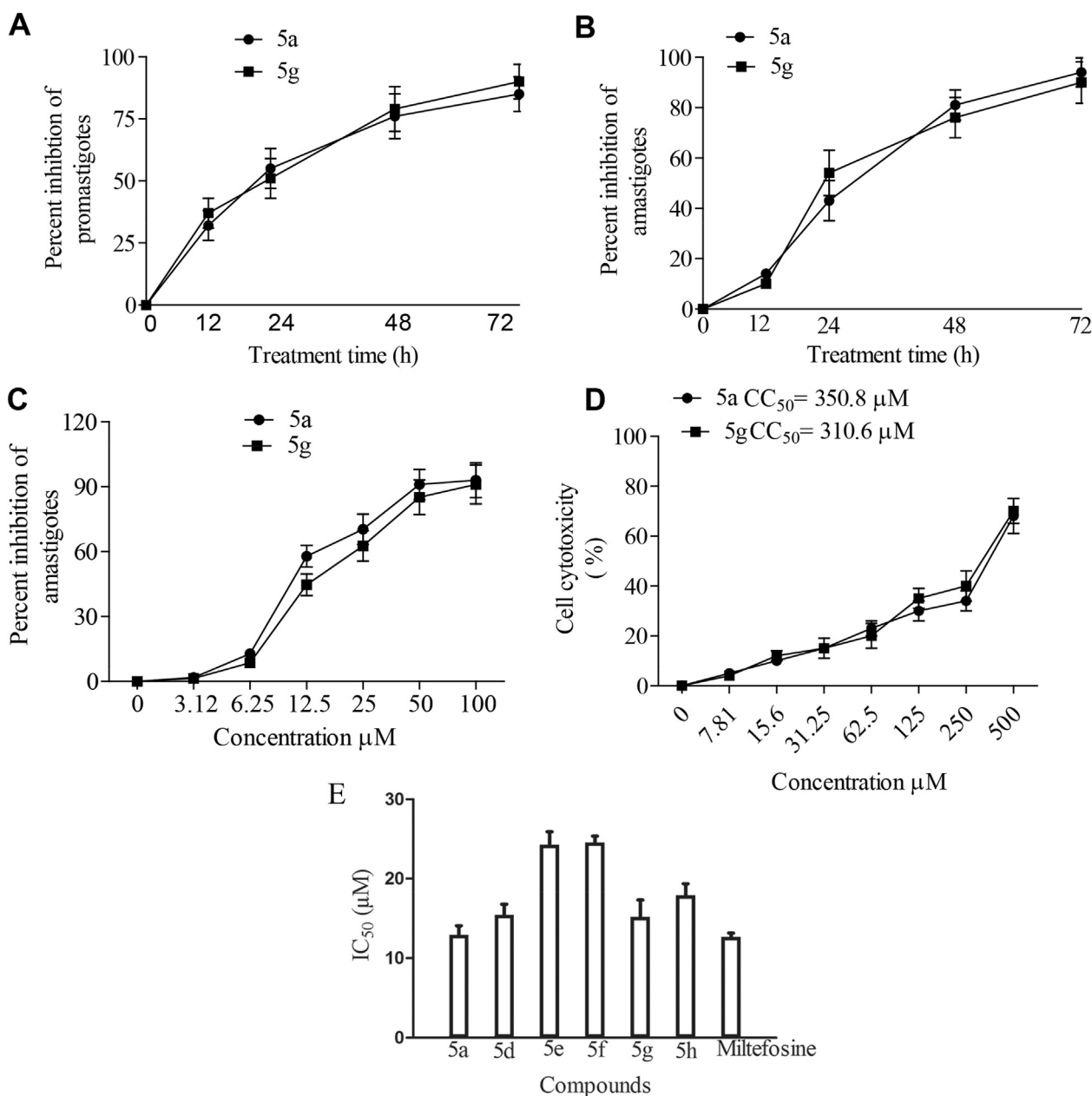


**Fig. 2.** *In vitro* anti-leishmanial efficacy of synthesized derivatives: (A) Percentage inhibition of **5a**- and **5g**-treated promastigotes by MTT assay as described in Experimental Section. (B) Percentage inhibition of **5a**- and **5g**-treated amastigotes by giemsa staining in J774 macrophages (C) Percentage inhibition of **5a**- and **5g**-treated amastigotes in J774 macrophages by luciferase assay as described in Experimental Section. (D) Determination of cellular cytotoxicity of **5a**- and **5g**-treated macrophages using MTT assay. (E) Determination of IC<sub>50</sub> of active compounds against intracellular amastigotes as described in Experimental Section.

compounds were characterised by spectroscopic techniques (<sup>1</sup>H NMR, <sup>13</sup>C NMR, ESMS, HRMS and IR) and were screened for anti-leishmanial activity. Among them, **5a** and **5g** showed better activity against intracellular amastigotes with an IC<sub>50</sub> of 11.07 μM and 15.3 μM, respectively. These two compounds further considered for anti-leishmanial activity in *in vivo* model for experimental visceral leishmaniasis. Additionally, we observed that compound **5a** showed more promising antileishmanial efficacy than **5g** in Balb/c model of VL. On a mechanistic view point, **5a** induced direct *Leishmania* killing by mitochondrial dysfunction like cytochrome c release and loss of membrane potential. Our results suggest that **5a** is a promising lead for further development of antileishmanial drugs. As it is important to continuously develop alternate solutions to decrease mortality rate caused by *Leishmania* parasite, our

study could constitute an opportunity for new derivatives for the treatment of fatal disease caused by *Leishmania* parasite.

## 4. Experimental Section

### 4.1. *In silico* study

The *in silico* analysis of the synthesized compounds was done by using free access Molinspiration [18] (<http://www.molinspiration.com>). For the theoretical study of toxicity (mutagenic, tumorigenic, and irritant effects) profiles of synthesized compounds **5a-q** and **7a-e**, the online web free OSIRIS Property Explorer [22] (<https://www.organic-chemistry.org/prog/peo/>) computer program was used.

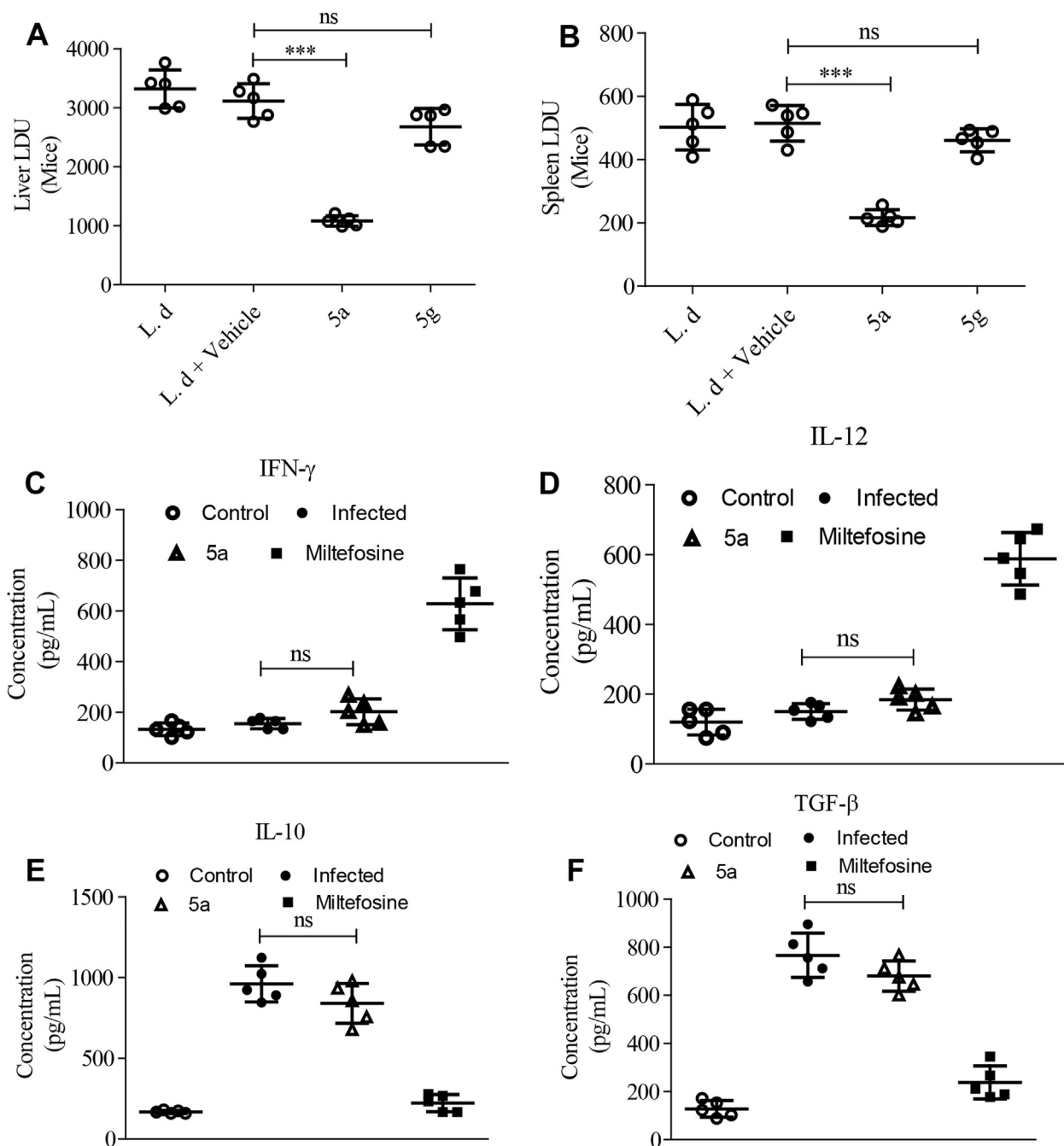


**Fig. 3.** Effect of **5a** and **5g** on *L. donovani* infected Balb/c mice. (A) liver and (B) spleen parasite burden were assessed in **5a**- and **5g**-treated Balb/c mice using stamps –smear method as described in Experimental Section. Miltefosine was used as a standard anti-leishmanial reference drug. The level of IFN- $\gamma$  (C), IL-12 (D), IL-10 (E) and TGF- $\beta$  (F) were determined in the supernatant harvested from splenocytes of different group of Balb/c mice as described in Experimental Section. Significance: infected vs infected + **5a** and infected + vehicle vs infected + **5a** ns, non significant, \* $p < 0.05$ , \*\* $p < 0.01$  and \*\*\* $p < 0.001$ .

## 4.2. Synthesis of compounds

### 4.2.1. General method for preparation of 2-(piperazin-1-yl)phenol substituted 2H-Pyranones **5a-q**

A mixture of 6-aryl-3-cyano-4-methylsulfanyl-2H-pyran-2-ones (**3a-h**, 1 mmol) and 2-(piperazin-1-yl)phenol (**4**, 1.2 mmol) was refluxed in methanol for 1–4 h. After completion, the reaction was cooled to room temperature and was filtered off and washed with methanol. Crude product was purified by silica gel column chromatography using 2% methanol in chloroform as eluent. Further for the synthesis of **5i**, a mixture of 4-(methylthio)-2-oxo-

2,5-dihydroindeno[1,2-*b*]pyran-3-carbonitrile and 2-(piperazin-1-yl)phenol (**4**, 1.2 mmol) was taken and for **5j** a mixture of 4-(methylthio)-2-oxo-5,6-dihydro-2H-benzo[*h*]chromene-3-carbonitrile and 2-(piperazin-1-yl)phenol (**4**, 1.2 mmol) was taken following the above method. Same procedure was followed for other derivatives.

### 4.2.2. General method for preparation of **7a-e**

A mixture of 6-(aryl)-4-(4-(2-hydroxyphenyl)piperazin-1-yl)-2-oxo-2H-pyran-3-carbonitrile (**5a,c,g,i**, 1 mmol, 1 equiv.), substituted acetophenones (**6a** and **6b**, 1.2 mmol, 1.2 equiv.), and

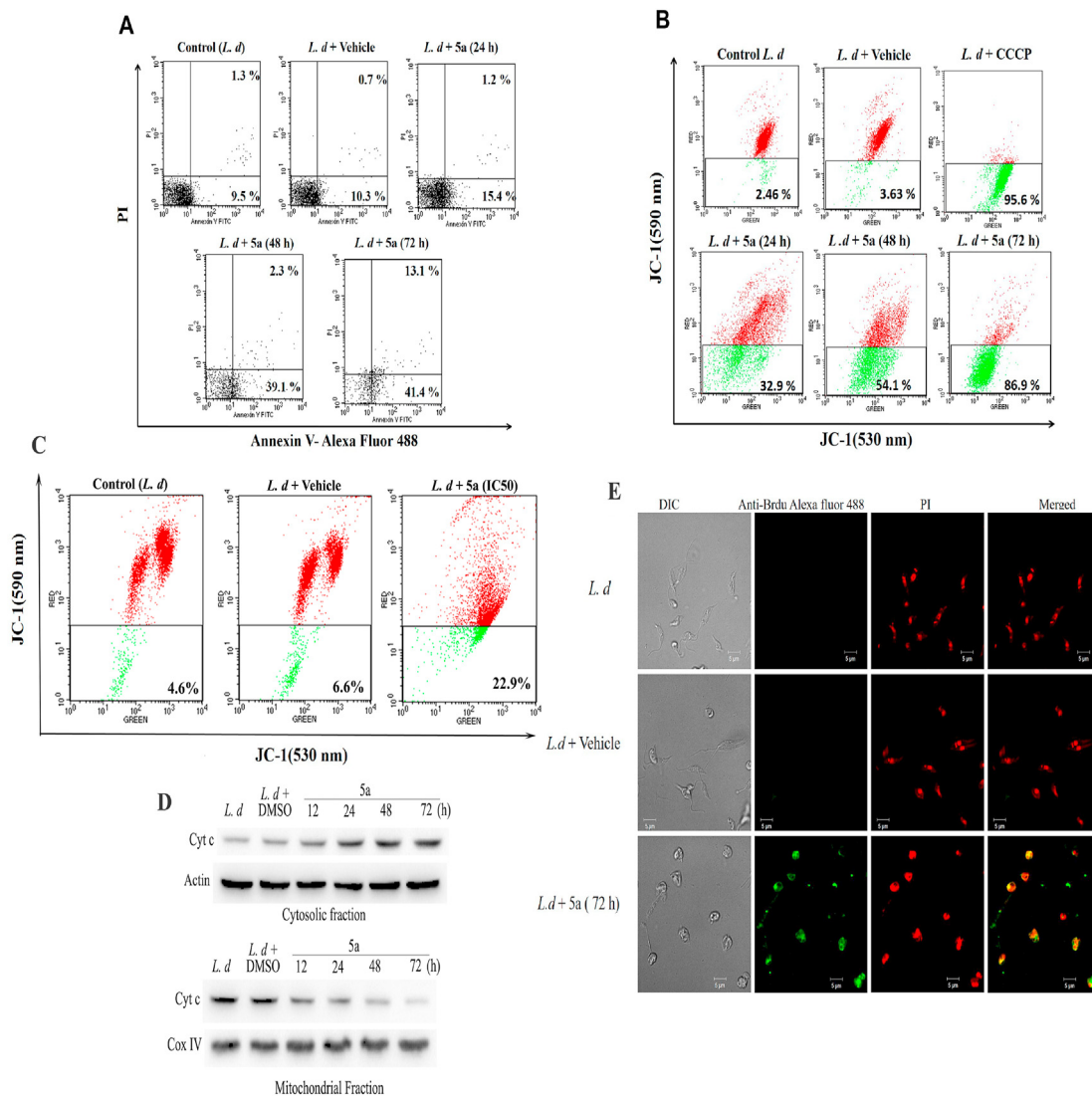


**Fig. 4.** 5a induces apoptosis cell death in *L. donovani* promastigotes via mitochondrial depolarization. (A) Flow cytometry analysis of Log phase *L. donovani* promastigotes treated with 50  $\mu\text{M}$  of 5a. Representative quadrant showing viable parasite (lower left as annexin V<sup>-</sup>PI<sup>-</sup>), early apoptotic (lower right as annexin V<sup>+</sup>PI<sup>-</sup>), late apoptotic (upper right as annexin V<sup>+</sup>PI<sup>+</sup>) and necrotic (upper left as annexin V<sup>+</sup>PI<sup>-</sup>). (B & C) Promastigotes were exposed to 50  $\mu\text{M}$  of 5a for 24–72 h or IC<sub>50</sub> of 5a for 72 h and then stained with JC-1 (2  $\mu\text{M}$ ). Loss in mitochondrial membrane potential was determined using flow cytometry. CCCP was used as a positive control. (D) Western blot for cytochrome c in mitochondria and cytosol fractions of *L. donovani* promastigotes treated with 50  $\mu\text{M}$  5a for 12–72 h. Actin was used as a loading control for cytosol fractions and COX-4 was used as a control for mitochondrial fractions. (E) Log phase promastigotes were treated with 50  $\mu\text{M}$  5a for 72 h. After fixation and permeabilization, non-treated and treated promastigotes were stained with labeling solution of Tdt enzyme and BrdUTP and analyzed by confocal microscopy.

KOH (2 mmol, 2 equiv.) in dry DMF (10 mL) was stirred at 25 °C for 1 h. The progress of the reaction was monitored by TLC and on completion the reaction mixture was poured onto crushed ice with vigorous stirring and finally neutralized with 10% HCl. The precipitate obtained was filtered and purified on a silica gel column using 5% ethyl acetate in hexane as the eluent.

#### 4.2.3. 4-(4-(2-hydroxyphenyl)piperazin-1-yl)-2-oxo-6-phenyl-2H-pyran-3-carbonitrile (5a)

Off-white solid, Yield 72%;  $R_f = 0.40$  (Chloroform/Methanol, 10:1, v/v); mp(Chloroform/Methanol): 267–269 °C; IR (KBr)  $\nu_{\text{max}} = 1702 \text{ cm}^{-1}$  (C=O str.),  $2210 \text{ cm}^{-1}$  (CN str.),  $3357 \text{ cm}^{-1}$  (OH str.); <sup>1</sup>H NMR (400 MHz, DMSO-*d*<sub>6</sub>):  $\delta = 3.11$  (t,  $J = 4.4 \text{ Hz}$ , 4H, 2NCH<sub>2</sub>), 4.08 (t,  $J = 4.2 \text{ Hz}$ , 4H, 2NCH<sub>2</sub>), 6.73–6.92 (m, 4H, Ar-H), 7.15 (s, 1H, C<sub>5</sub>-H), 7.53–7.59 (m, 3H, Ar-H), 7.98–8.00 (m, 2H, Ar-H), 9.11 (s, 1H, OH) ppm; <sup>13</sup>C NMR (100.6 MHz, DMSO-*d*<sub>6</sub>):  $\delta = 49.8, 50.8, 71.2, 79.6, 96.2, 116.2, 118.1, 119.6, 119.9, 124.1, 126.8, 129.5, 131.0, 132.2,$

139.1, 150.7, 159.8, 161.0, 162.3 ppm; MS (ESI) 374 [M + H]<sup>+</sup>; HRMS calculated for C<sub>22</sub>H<sub>20</sub>N<sub>3</sub>O<sub>3</sub> [M + H]<sup>+</sup> 374.1505, found: 374.1494.

#### 4.2.4. 6-(4-chlorophenyl)-4-(4-(2-hydroxyphenyl)piperazin-1-yl)-2-oxo-2H-pyran-3-carbonitrile (5b)

Light yellow; Yield 68%;  $R_f = 0.38$  (Chloroform/Methanol, 10:1, v/v); mp(Chloroform/Methanol): 283–285 °C; IR (KBr)  $\nu_{\text{max}} = 1682 \text{ cm}^{-1}$  (C=O str.),  $2210 \text{ cm}^{-1}$  (CN str.),  $3351 \text{ cm}^{-1}$  (OH str.); <sup>1</sup>H NMR (400 MHz, DMSO-*d*<sub>6</sub>):  $\delta = 3.11$  (t,  $J = 4.4 \text{ Hz}$ , 4H, 2NCH<sub>2</sub>), 4.08 (t,  $J = 4.2 \text{ Hz}$ , 4H, 2NCH<sub>2</sub>), 6.73–6.92 (m, 4H, Ar-H), 7.18 (s, 1H, C<sub>5</sub>-H), 7.63 (d,  $J = 8.8 \text{ Hz}$ , 2H, Ar-H), 8.02 (d,  $J = 8.8 \text{ Hz}$ , 2H, Ar-H), 9.10 (s, 1H, OH) ppm; <sup>13</sup>C NMR (100.6 MHz, DMSO-*d*<sub>6</sub>):  $\delta = 49.9, 50.8, 71.3, 96.6, 116.2, 118.1, 119.6, 120.0, 124.1, 128.6, 129.6, 129.9, 137.0, 139.2, 150.7, 158.6, 160.9, 162.2 \text{ ppm}$ ; MS (ESI) 408 [M + H]<sup>+</sup>, 410 [M + 2 + H]<sup>+</sup>; HRMS calculated for C<sub>22</sub>H<sub>19</sub>ClN<sub>3</sub>O<sub>3</sub> [M + H]<sup>+</sup> 408.1115, found: 408.1103 and [M + 2 + H]<sup>+</sup> 410.1085, found: 410.1074.

#### 4.2.5. 6-(4-bromophenyl)-4-(4-(2-hydroxyphenyl)piperazin-1-yl)-2-oxo-2H-pyran-3-carbonitrile (**5c**)

Light yellow; Yield 66%;  $R_f = 0.40$  (Chloroform/Methanol, 10:1, v/v); mp(Chloroform/Methanol): 281–283 °C; IR (KBr)  $\nu_{\max} = 1684 \text{ cm}^{-1}$  (C=O str.), 2210  $\text{cm}^{-1}$  (CN str.), 3350 (OH str.);  $^1\text{H}$  NMR (400 MHz, DMSO- $d_6$ ):  $\delta = 3.11$  (s, 4H, 2NCH<sub>2</sub>), 4.08 (s, 4H, 2NCH<sub>2</sub>), 6.74–6.91 (m, 4H, Ar–H), 7.20 (s, 1H, C<sub>5</sub>–H), 7.77 (d,  $J = 8.7$  Hz, 2H, Ar–H), 7.95 (d,  $J = 8.7$  Hz, 2H, Ar–H), 9.11 (s, 1H, OH) ppm;  $^{13}\text{C}$  NMR (100.6 MHz, DMSO- $d_6$ ):  $\delta = 49.9, 50.9, 71.4, 96.7, 116.3, 118.2, 119.7, 120.1, 124.2, 126.1, 128.8, 130.3, 132.6, 139.2, 150.8, 158.8, 151.0, 162.3$  ppm; MS (ESI) 452 [M + H]<sup>+</sup>, 454 [M + 2 + H]<sup>+</sup>; HRMS calculated for C<sub>22</sub>H<sub>19</sub>BrN<sub>3</sub>O<sub>3</sub> [M + H]<sup>+</sup> 452.0610, found: 452.0604, [M + 2 + H]<sup>+</sup> 454.0589, found: 454.0584.

#### 4.2.6. 4-(4-(2-hydroxyphenyl)piperazin-1-yl)-2-oxo-6-(p-tolyl)-2H-pyran-3-carbonitrile (**5d**)

Light yellow; Yield 62%;  $R_f = 0.37$  (Chloroform/Methanol, 10:1, v/v); mp(Chloroform/Methanol): 288–290 °C; IR (KBr)  $\nu_{\max} = 1682 \text{ cm}^{-1}$  (C=O str.), 2203  $\text{cm}^{-1}$  (CN str.), 3381 (OH str.);  $^1\text{H}$  NMR (400 MHz, DMSO- $d_6$ ):  $\delta = 2.39$  (s, 3H, CH<sub>3</sub>), 3.11 (s, 4H, 2NCH<sub>2</sub>), 4.08 (s, 4H, 2NCH<sub>2</sub>), 6.74–6.92 (m, 4H, Ar–H), 7.10 (s, 1H, C<sub>5</sub>–H), 7.37 (d,  $J = 8.1$  Hz, 2H, Ar–H), 7.90 (d,  $J = 8.2$  Hz, 2H, Ar–H), 9.11 (s, 1H, OH) ppm;  $^{13}\text{C}$  NMR (100.6 MHz, DMSO- $d_6$ ):  $\delta = 21.5, 49.7, 50.7, 71.0, 95.3, 116.2, 118.2, 119.6, 124.0, 126.7, 128.2, 130.0, 139.1, 142.5, 150.7, 160.0, 161.1, 162.3$  ppm; MS (ESI) 388 [M + H]<sup>+</sup>; HRMS calculated for C<sub>23</sub>H<sub>22</sub>N<sub>3</sub>O<sub>3</sub> [M + H]<sup>+</sup> 388.1661, found: 388.1651.

#### 4.2.7. 4-(4-(2-hydroxyphenyl)piperazin-1-yl)-6-(4-methoxyphenyl)-2-oxo-2H-pyran-3-carbonitrile (**5e**)

Light yellow; Yield 61%;  $R_f = 0.32$  (Chloroform/Methanol, 10:1, v/v); mp(Chloroform/Methanol): 250–252 °C; IR (KBr)  $\nu_{\max} = 1687 \text{ cm}^{-1}$  (C=O str.), 2203  $\text{cm}^{-1}$  (CN str.), 3377 (OH str.);  $^1\text{H}$  NMR (400 MHz, DMSO- $d_6$ ):  $\delta = 3.11$  (t,  $J = 4.4$  Hz, 4H, 2NCH<sub>2</sub>), 3.84 (s, 3H, OMe), 4.06 (t,  $J = 4.2$  Hz, 4H, 2NCH<sub>2</sub>), 6.73–6.91 (m, 4H, Ar–H), 7.02 (s, 1H, C<sub>5</sub>–H), 7.09 (d,  $J = 8.9$  Hz, 2H, Ar–H), 7.96 (d,  $J = 8.9$  Hz, 2H, Ar–H), 9.10 (s, 1H, OH) ppm;  $^{13}\text{C}$  NMR (100.6 MHz, DMSO- $d_6$ ):  $\delta = 49.8, 50.8, 56.0, 70.6, 94.4, 115.0, 116.2, 118.3, 119.6, 120.0, 123.2, 124.1, 128.7, 139.2, 150.7, 160.0, 161.3, 162.5, 162.6$  ppm; MS (ESI) 404 [M + H]<sup>+</sup>; HRMS calculated for C<sub>23</sub>H<sub>22</sub>N<sub>3</sub>O<sub>4</sub> [M + H]<sup>+</sup> 404.1610, found: 404.1606.

#### 4.2.8. 4-(4-(2-hydroxyphenyl)piperazin-1-yl)-6-(naphthalen-1-yl)-2-oxo-2H-pyran-3-carbonitrile (**5f**)

Off white solid; Yield 58%;  $R_f = 0.36$  (Chloroform/Methanol, 10:1, v/v); mp(Chloroform/Methanol): 247–248 °C; IR (KBr)  $\nu_{\max} = 1702 \text{ cm}^{-1}$  (C=O str.), 2211  $\text{cm}^{-1}$  (CN str.), 3369 (OH str.);  $^1\text{H}$  NMR (400 MHz, DMSO- $d_6$ ):  $\delta = 3.11$  (t,  $J = 4.4$  Hz, 4H, 2NCH<sub>2</sub>), 4.07 (t,  $J = 4.4$  Hz, 4H, 2NCH<sub>2</sub>), 6.75–6.91 (m, 4H, Ar–H), 6.99 (s, 1H, C<sub>5</sub>–H), 7.62–7.66 (m, 3H, Ar–H), 7.80–7.82 (m, 1H, Ar–H), 8.04–8.16 (m, 3H, Ar–H), 9.10 (s, 1H, OH) ppm;  $^{13}\text{C}$  NMR (100.6 MHz, DMSO- $d_6$ ):  $\delta = 49.8, 50.7, 71.3, 101.1, 116.2, 118.2, 119.6, 124.1, 125.3, 125.7, 127.1, 128.0, 128.9, 129.1, 130.0, 130.2, 131.9, 133.6, 139.1, 150.7, 160.9, 161.9, 162.7$  ppm; MS (ESI) 424 [M + H]<sup>+</sup>; HRMS calculated for C<sub>26</sub>H<sub>22</sub>N<sub>3</sub>O<sub>3</sub> [M + H]<sup>+</sup> 424.1661, found: 424.1654.

#### 4.2.9. 4-(4-(2-hydroxyphenyl)piperazin-1-yl)-2-oxo-6-(thiophen-2-yl)-2H-pyran-3-carbonitrile (**5g**)

Brown solid; Yield 55%;  $R_f = 0.31$  (Chloroform/Methanol, 10:1, v/v); mp(Chloroform/Methanol): 248–250 °C; IR (KBr)  $\nu_{\max} = 1706 \text{ cm}^{-1}$  (C=O str.), 2205  $\text{cm}^{-1}$  (CN str.), 3399 (OH str.);  $^1\text{H}$  NMR (400 MHz, DMSO- $d_6$ ):  $\delta = 3.10$  (t,  $J = 4.4$  Hz, 4H, 2NCH<sub>2</sub>), 4.05 (t,  $J = 4.2$  Hz, 4H, 2NCH<sub>2</sub>), 6.73–6.92 (m, 4H, Ar–H), 7.07 (s, 1H, C<sub>5</sub>–H), 7.27–7.29 (m, 1H, Ar–H), 7.93–7.94 (m, 1H, Ar–H), 8.04–8.05 (m, 1H, Ar–H), 9.11 (s, 1H, OH) ppm;  $^{13}\text{C}$  NMR (100.6 MHz, DMSO- $d_6$ ):  $\delta = 49.8, 50.7, 70.6, 94.4, 116.2, 118.2, 119.6,$

120.0, 124.1, 129.5, 130.2, 132.4, 134.4, 139.2, 150.7, 155.9, 160.9, 161.8 ppm; MS (ESI) 380 [M + H]<sup>+</sup>; HRMS calculated for C<sub>20</sub>H<sub>18</sub>N<sub>3</sub>O<sub>3</sub>S [M + H]<sup>+</sup> 380.1069, found: 380.1057.

#### 4.2.10. 6-(5-Bromothiophen-2-yl)-4-(4-(2-hydroxyphenyl)piperazin-1-yl)-2-oxo-2H-pyran-3-carbonitrile (**5h**)

Yellow solid; Yield 50%;  $R_f = 0.35$  (Chloroform/Methanol, 10:1, v/v); mp(Chloroform/Methanol): 274–276 °C; IR (KBr)  $\nu_{\max} = 1716 \text{ cm}^{-1}$  (C=O str.), 2201  $\text{cm}^{-1}$  (CN str.), 3338 (OH str.);  $^1\text{H}$  NMR (400 MHz, DMSO- $d_6$ ):  $\delta = 3.10$  (s, 4H, 2NCH<sub>2</sub>), 4.04 (s, 4H, 2NCH<sub>2</sub>), 6.73–6.91 (m, 4H, Ar–H), 7.09 (s, 1H, C<sub>5</sub>–H), 7.44 (d,  $J = 4.1$  Hz, 1H, Ar–H), 7.89 (d,  $J = 4.1$  Hz, 1H, Ar–H), 9.10 (s, 1H, OH) ppm;  $^{13}\text{C}$  NMR (100.6 MHz, DMSO- $d_6$ ):  $\delta = 49.9, 50.7, 70.8, 94.7, 116.2, 118.1, 119.6, 120.0, 124.1, 130.7, 132.9, 135.8, 139.1, 145.8, 150.7, 154.5, 160.7, 161.6$  ppm; MS (ESI) 458 [M + H]<sup>+</sup>, 460 [M + 2 + H]<sup>+</sup>; HRMS calculated for C<sub>20</sub>H<sub>17</sub>BrN<sub>3</sub>O<sub>3</sub>S [M + H]<sup>+</sup> 458.0174, found: 458.0167 and [M + 2 + H]<sup>+</sup> 460.0154, found: 460.0139.

#### 4.2.11. 4-(4-(2-hydroxyphenyl)piperazin-1-yl)-2-oxo-2,5-dihydroindeno[1,2-b]pyran-3-carbonitrile (**5i**)

Brown solid; Yield 47%;  $R_f = 0.40$  (Chloroform/Methanol, 10:1, v/v); mp(Chloroform/Methanol): 258–260 °C; IR (KBr)  $\nu_{\max} = 1732 \text{ cm}^{-1}$  (C=O str.), 2202  $\text{cm}^{-1}$  (CN str.), 3353 (OH str.);  $^1\text{H}$  NMR (400 MHz, DMSO- $d_6$ ):  $\delta = 3.17$  (t,  $J = 4.4$  Hz, 4H, 2NCH<sub>2</sub>), 4.02 (t,  $J = 4.3$  Hz, 4H, 2NCH<sub>2</sub>), 4.14 (s, 2H, Ar–CH<sub>2</sub>), 6.74–6.94 (m, 4H, Ar–H), 7.49–7.58 (m, 2H, Ar–H), 7.66–7.71 (m, 2H, Ar–H), 9.13 (s, 1H, OH) ppm;  $^{13}\text{C}$  NMR (100.6 MHz, DMSO- $d_6$ ):  $\delta = 36.3, 51.2, 72.9, 112.1, 116.4, 118.7, 119.8, 120.2, 120.7, 124.4, 125.6, 128.4, 131.0, 133.8, 139.3, 144.0, 150.8, 162.3, 162.8$  ppm; MS (ESI) 386 [M + H]<sup>+</sup>; HRMS calculated for C<sub>23</sub>H<sub>20</sub>N<sub>3</sub>O<sub>3</sub> [M + H]<sup>+</sup> 386.1505, found: 386.1498.

#### 4.2.12. 4-(4-(2-hydroxyphenyl)piperazin-1-yl)-2-oxo-5,6-dihydro-2H-benzo[h]chromene-3-carbonitrile (**5j**)

Dark Yellow solid; Yield 44%;  $R_f = 0.40$  (Chloroform/Methanol, 10:1, v/v); mp(Chloroform/Methanol): 260–262 °C; IR (KBr)  $\nu_{\max} = 1730 \text{ cm}^{-1}$  (C=O str.), 2210  $\text{cm}^{-1}$  (CN str.), 3357 (OH str.);  $^1\text{H}$  NMR (400 MHz, DMSO- $d_6$ ):  $\delta = 2.73$ –2.77 (m, 2H, CH<sub>2</sub>), 2.85–2.88 (m, 2H, CH<sub>2</sub>), 3.12 (s, 4H, 2NCH<sub>2</sub>), 3.73 (s, 4H, 2NCH<sub>2</sub>), 6.74–6.94 (m, 4H, Ar–H), 7.35–7.48 (m, 3H, Ar–H), 7.68 (d,  $J = 6.84$ , 1H, Ar–H), 9.11 (s, 1H, OH) ppm;  $^{13}\text{C}$  NMR (100.6 MHz, DMSO- $d_6$ ):  $\delta = 23.5, 27.7, 51.4, 52.1, 79.7, 110.3, 116.5, 118.0, 119.9, 120.4, 124.3, 124.4, 128.1, 128.3, 128.5, 132.3, 139.1, 139.8, 150.9, 156.8, 161.8, 167.2$  ppm; MS (ESI) 400 [M + H]<sup>+</sup>; HRMS calculated for C<sub>24</sub>H<sub>22</sub>N<sub>3</sub>O<sub>3</sub> [M + H]<sup>+</sup> 400.1661, found: 415.1658.

#### 4.2.13. 4-(4-(2-chlorophenyl)piperazin-1-yl)-2-oxo-6-phenyl-2H-pyran-3-carbonitrile (**5k**)

Yellow solid; Yield 62%;  $R_f = 0.35$  (Chloroform/Methanol, 10:1, v/v); mp(Chloroform/Methanol): 216–214 °C; IR (KBr)  $\nu_{\max} = 1700 \text{ cm}^{-1}$  (C=O str.), 2207  $\text{cm}^{-1}$  (CN str.);  $^1\text{H}$  NMR (400 MHz, DMSO- $d_6$ ):  $\delta = 3.18$  (t,  $J = 4.8$  Hz, 4H, 2NCH<sub>2</sub>), 4.08 (t,  $J = 4.8$  Hz, 4H, 2NCH<sub>2</sub>), 7.08–7.13 (m, 1H, Ar–H), 7.17–7.21 (m, 2H, Ar–H), 7.31–7.36 (m, 1H, Ar–H), 7.46 (dd,  $J_1 = 7.9, J_2 = 1.5$  Hz, 1H, Ar–H), 7.56–7.59 (m, 3H, Ar–H), 7.99–8.01 (m, 2H, Ar–H) ppm;  $^{13}\text{C}$  NMR (100.6 MHz, DMSO- $d_6$ ):  $\delta = 49.8, 51.3, 71.6, 96.3, 118.1, 121.7, 125.0, 126.8, 128.1, 128.7, 129.5, 130.9, 131.0, 132.3, 148.4, 159.9, 161.3, 162.3$  ppm; MS (ESI) 392 [M + H]<sup>+</sup>; HRMS calculated for C<sub>22</sub>H<sub>18</sub>ClN<sub>3</sub>O<sub>3</sub> [M + H]<sup>+</sup> 392.1166, found: 392.1158.

#### 4.2.14. 6-(4-chlorophenyl)-4-(4-(2-chlorophenyl)piperazin-1-yl)-2-oxo-2H-pyran-3-carbonitrile (**5l**)

White solid; Yield 55%;  $R_f = 0.40$  (Chloroform/Methanol, 10:1, v/v); mp(Chloroform/Methanol): 234–236 °C; IR (KBr)  $\nu_{\max} = 1699 \text{ cm}^{-1}$  (C=O str.), 2205  $\text{cm}^{-1}$  (CN str.);  $^1\text{H}$  NMR (400 MHz, DMSO- $d_6$ ):  $\delta = 3.18$  (t,  $J = 4.9$  Hz, 4H, 2NCH<sub>2</sub>), 4.10 (t,

$J = 4.9$  Hz, 4H, 2NCH<sub>2</sub>), 7.10 (td,  $J_1 = 7.6$ ,  $J_2 = 1.5$  Hz, 1H, Ar–H), 7.18–7.21 (m, 2H, Ar–H), 7.31–7.36 (m, 1H, Ar–H), 7.46 (dd,  $J_1 = 7.9$ ,  $J_2 = 1.5$  Hz, 1H, Ar–H), 7.63–7.65 (m, 2H, Ar–H), 8.02–8.04 (m, 2H, Ar–H) ppm; <sup>13</sup>C NMR (100.6 MHz, DMSO-*d*<sub>6</sub>):  $\delta = 49.8$ , 51.3, 71.7, 96.7, 118.0, 121.7, 125.0, 128.2, 128.6, 129.6, 129.8, 130.9, 137.1, 148.4, 158.7, 161.2, 162.0 ppm; MS (ESI) 426 [M + H]<sup>+</sup>; HRMS calculated for C<sub>22</sub>H<sub>17</sub>Cl<sub>2</sub>N<sub>3</sub>O<sub>2</sub> [M + H]<sup>+</sup> 426.0776, found: 426.0772.

#### 4.2.15. 6-(4-bromophenyl)-4-(4-(2-chlorophenyl)piperazin-1-yl)-2-oxo-2H-pyran-3-carbonitrile (**5m**)

White solid; Yield 50%;  $R_f = 0.25$  (Chloroform/Methanol, 10:1, v/v); mp(Chloroform/Methanol): 240–242 °C; IR (KBr)  $\nu_{\max} = 1684$  cm<sup>-1</sup> (C=O str.), 2205 cm<sup>-1</sup> (CN str.); <sup>1</sup>H NMR (400 MHz, DMSO-*d*<sub>6</sub>):  $\delta = 3.18$  (t,  $J = 4.8$  Hz, 4H, 2NCH<sub>2</sub>), 4.10 (t,  $J = 4.8$  Hz, 4H, 2NCH<sub>2</sub>), 7.08–7.12 (m, 2H, Ar–H), 7.18–7.22 (m, 1H, Ar–H), 7.32–7.35 (m, 1H, Ar–H), 7.45–7.47 (m, 1H, Ar–H), 7.76–7.79 (m, 2H, Ar–H), 7.94–7.97 (m, 2H, Ar–H) ppm; <sup>13</sup>C NMR (100.6 MHz, DMSO-*d*<sub>6</sub>):  $\delta = 49.8$ , 51.3, 71.7, 96.7, 118.0, 121.7, 125.0, 126.0, 128.1, 128.7, 128.8, 130.1, 130.9, 132.5, 148.4, 158.7, 161.2, 162.0 ppm; MS (ESI) 470 [M + H]<sup>+</sup>, 472 [M + 2 + H]<sup>+</sup>; HRMS calculated for C<sub>22</sub>H<sub>17</sub>BrClN<sub>3</sub>O<sub>2</sub> [M + H]<sup>+</sup> 470.0271, found: 470.0221 and [M + 2 + H]<sup>+</sup> 472.0271, found: 472.0194.

#### 4.2.16. 4-(4-(2-chlorophenyl)piperazin-1-yl)-6-(4-methoxyphenyl)-2-oxo-2H-pyran-3-carbonitrile (**5n**)

White solid; Yield 50%;  $R_f = 0.37$  (Chloroform/Methanol, 10:1, v/v); mp(Chloroform/Methanol): 200–202 °C; IR (KBr)  $\nu_{\max} = 1698$  cm<sup>-1</sup> (C=O str.), 2205 cm<sup>-1</sup> (CN str.), 3410 (OH str.); <sup>1</sup>H NMR (400 MHz, DMSO-*d*<sub>6</sub>):  $\delta = 3.17$  (t,  $J = 4.8$  Hz, 4H, 2NCH<sub>2</sub>), 3.86 (s, 3H, OMe), 4.08 (t,  $J = 4.8$  Hz, 4H, 2NCH<sub>2</sub>), 7.04 (s, 1H, C<sub>5</sub>–H), 7.08–7.12 (m, 3H, Ar–H), 7.20 (dd,  $J_1 = 8.1$ ,  $J_2 = 1.6$  Hz, 1H, Ar–H), 7.31–7.35 (m, 1H, Ar–H), 7.46 (dd,  $J_1 = 7.9$ ,  $J_2 = 1.5$  Hz, 1H, Ar–H), 7.96–7.98 (m, 2H, Ar–H) ppm; <sup>13</sup>C NMR (100.6 MHz, DMSO-*d*<sub>6</sub>):  $\delta = 49.7$ , 51.3, 56.1, 70.9, 94.5, 114.9, 118.2, 121.7, 123.1, 125.0, 128.1, 128.7, 128.8, 130.9, 148.4, 160.1, 161.6, 162.3, 162 ppm; MS (ESI) 422 [M + H]<sup>+</sup>; HRMS calculated for C<sub>23</sub>H<sub>20</sub>ClN<sub>3</sub>O<sub>3</sub> [M + H]<sup>+</sup> 422.1271, found: 422.1269.

#### 4.2.17. 4-(4-(3-chlorophenyl)piperazin-1-yl)-2-oxo-6-phenyl-2H-pyran-3-carbonitrile (**5o**)

White solid; Yield 50%;  $R_f = 0.37$  (Chloroform/Methanol, 10:1, v/v); mp(Chloroform/Methanol): 200–202 °C; IR (KBr)  $\nu_{\max} = 1698$  cm<sup>-1</sup> (C=O str.), 2205 cm<sup>-1</sup> (CN str.), 3410 (OH str.); <sup>1</sup>H NMR (400 MHz, CDCl<sub>3</sub>):  $\delta = 3.49$ –3.44 (m, 4H, 2NCH<sub>2</sub>), 4.12–4.06 (m, 4H, 2NCH<sub>2</sub>), 6.51 (s, 1H, C<sub>5</sub>–H), 6.77–6.82 (m, 1H, Ar–H), 6.94–6.88 (m, 2H, Ar–H), 7.20–7.26 (m, 1H, Ar–H), 7.57–7.48 (m, 3H, Ar–H), 7.88–7.81 (m, 2H, Ar–H) ppm; <sup>13</sup>C NMR (100.6 MHz, CDCl<sub>3</sub>):  $\delta = 48.3$ , 48.8, 94.2, 113.7, 115.7, 117.1, 120.3, 126.3, 129.1, 130.3, 130.5, 132.1, 135.2, 150.9, 161.1, 161.6, 161.9 ppm; MS (ESI) 392.05 [M + H]<sup>+</sup>; HRMS calculated for C<sub>22</sub>H<sub>19</sub>ClN<sub>3</sub>O<sub>2</sub> [M + H]<sup>+</sup> 422.1271, found: 422.1269.

#### 4.2.18. 4-(4-(2-methoxyphenyl)piperazin-1-yl)-2-oxo-6-(thiophen-2-yl)-2H-pyran-3-carbonitrile (**5p**)

Off White solid; Yield 68%;  $R_f = 0.35$  (Chloroform/Methanol, 10:1, v/v); mp(Chloroform/Methanol): 242–243 °C; IR (KBr)  $\nu_{\max} = 1700$  cm<sup>-1</sup> (C=O str.), 2205 cm<sup>-1</sup> (CN str.); <sup>1</sup>H NMR (400 MHz, CDCl<sub>3</sub>):  $\delta = 3.3$ –3.2 (m, 4H, 2NCH<sub>2</sub>), 3.90 (s, 3H, OMe), 4.05 (t,  $J = 5.0$  Hz, 4H, 2NCH<sub>2</sub>), 6.34 (s, 1H, C<sub>5</sub>–H), 6.98–6.88 (m, 3H, Ar–H), 7.09–7.04 (m, 1H, Ar–H), 7.16–7.12 (m, 1H, Ar–H), 7.55 (dd,  $J = 5.0$ , 1.2 Hz, 1H, Ar–H), 7.69 (dd,  $J = 3.8$ , 1.2 Hz, 1H, Ar–H) ppm; <sup>13</sup>C NMR (100.6 MHz, CDCl<sub>3</sub>):  $\delta = 49.7$ , 50.6, 55.4, 72.6, 93.1, 111.4, 117.3, 118.5, 121.1, 124.0, 128.7, 129.5, 130.6, 134.1, 139.6, 152.2, 156.7, 160.9, 161.6 ppm; MS (ESI) 394 [M + H]<sup>+</sup>; HRMS calculated for C<sub>21</sub>H<sub>20</sub>N<sub>3</sub>O<sub>3</sub>S [M + H]<sup>+</sup> 394.1225, found: 394.1216.

#### 4.2.19. 6-(4-bromophenyl)-4-(4-(2-methoxyphenyl)piperazin-1-yl)-2-oxo-2H-pyran-3-carbonitrile (**5q**)

Light yellow solid; Yield 64%;  $R_f = 0.37$  (Chloroform/Methanol, 10:1, v/v); mp(Chloroform/Methanol): 246–247 °C; IR (KBr)  $\nu_{\max} = 1697$  cm<sup>-1</sup> (C=O str.), 2205 cm<sup>-1</sup> (CN str.); <sup>1</sup>H NMR (400 MHz, CDCl<sub>3</sub>):  $\delta = 3.27$  (t,  $J = 4.9$  Hz, 4H, 2NCH<sub>2</sub>), 3.90 (s, 3H, OMe), 4.07 (t,  $J = 5.0$  Hz, 4H, 2NCH<sub>2</sub>), 6.50 (s, 1H, C<sub>5</sub>–H), 6.98–6.88 (m, 3H, Ar–H), 7.10–7.04 (m, 1H, Ar–H), 7.66–7.59 (m, 2H, Ar–H), 7.72–7.66 (m, 2H, Ar–H) ppm; <sup>13</sup>C NMR (100.6 MHz, CDCl<sub>3</sub>):  $\delta = 49.7$ , 50.6, 55.4, 73.3, 94.6, 111.5, 117.0, 118.6, 121.2, 124.1, 126.8, 127.6, 129.5, 132.4, 139.5, 152.2, 160.2, 160.7, 161.8 ppm; MS (ESI) 466 [M + H]<sup>+</sup>; HRMS calculated for C<sub>23</sub>H<sub>21</sub>BrN<sub>3</sub>O<sub>3</sub> [M + H]<sup>+</sup> 466.0766, found: 466.0757 [M + H]<sup>+</sup> and 468.0736 [M + 2 + H]<sup>+</sup>.

#### 4.2.20. 5-(4-(2-hydroxyphenyl)piperazin-1-yl)-7-phenyl-2,3-dihydrobenzo[b]thiophene-4-carbonitrile (**7a**)

Greenish yellow solid; Yield 55%;  $R_f = 0.45$  (Ethylacetate/Hexane, 1:20, v/v); mp(Ethylacetate/Hexane): 175–177 °C; IR (KBr)  $\nu_{\max} = 2210$  cm<sup>-1</sup> (CN str.); <sup>1</sup>H NMR (400 MHz, CDCl<sub>3</sub>):  $\delta = 3.10$  (t,  $J = 4.4$  Hz, 4H, 2NCH<sub>2</sub>), 3.33–3.39 (m, 6H, 2NCH<sub>2</sub>, SCH 2), 3.54–3.58 (m, 2H, SCH 2), 6.87–6.91 (m, 2H, Ar–H), 6.95–6.97 (m, 1H, Ar–H), 7.08–7.12 (m, 1H, Ar–H), 7.24–7.27 (m, 2H, Ar–H), 7.39–7.53 (m, 5H, Ar–H) ppm; <sup>13</sup>C NMR (100.6 MHz, CDCl<sub>3</sub>):  $\delta = 32.4$ , 36.9, 52.7, 52.9, 103.0, 114.1, 117.0, 118.5, 120.2, 121.7, 126.7, 127.7, 128.5, 128.7, 135.0, 138.5, 139.8, 140.6, 146.5, 151.4, 152.9 ppm; MS (ESI) 414 [M + H]<sup>+</sup>; HRMS calculated for C<sub>25</sub>H<sub>24</sub>N<sub>3</sub>OS [M + H]<sup>+</sup> 414.1640, found: 414.1623.

#### 4.2.21. 5-(4-(2-hydroxyphenyl)piperazin-1-yl)-7-(thiophen-2-yl)-2,3-dihydrobenzo[b]thiophene-4-carbonitrile (**7b**)

Pale yellow solid; Yield 50%;  $R_f = 0.40$  (Ethylacetate/Hexane, 1:20, v/v); mp(Ethylacetate/Hexane): 193–195 °C; IR (KBr)  $\nu_{\max} = 2218$  cm<sup>-1</sup> (CN str.); <sup>1</sup>H NMR (400 MHz, CDCl<sub>3</sub>):  $\delta = 3.10$  (t,  $J = 4.4$  Hz, 4H, 2NCH<sub>2</sub>), 3.34 (t,  $J = 4.4$  Hz, 4H, 2NCH<sub>2</sub>), 3.42–3.46 (m, 2H, SCH 2), 3.53–3.57 (m, 2H, SCH 2), 6.87–6.92 (m, 1H, Ar–H), 6.96–6.98 (m, 1H, Ar–H), 7.07–7.11 (m, 2H, Ar–H), 7.12–7.16 (m, 1H, Ar–H), 7.24–7.27 (m, 2H, Ar–H), 7.41–7.43 (m, 1H, Ar–H), 7.47–7.48 (m, 1H, Ar–H) ppm; <sup>13</sup>C NMR (100.6 MHz, CDCl<sub>3</sub>):  $\delta = 32.7$ , 36.8, 52.6, 52.7, 102.7, 114.1, 116.9, 117.3, 120.2, 121.7, 126.7, 127.0, 128.0, 133.2, 133.8, 138.5, 141.5, 147.2, 151.4, 152.6 ppm; MS (ESI) 420 [M + H]<sup>+</sup>; HRMS calculated for C<sub>23</sub>H<sub>22</sub>N<sub>3</sub>O<sub>2</sub> [M + H]<sup>+</sup> 420.1204, found: 420.1194.

#### 4.2.22. 5-(4-(2-hydroxyphenyl)piperazin-1-yl)-3,6-dihydro-2H-fluoreno[4,3-*b*]thiophene-4-carbonitrile (**7c**)

Pale yellow solid; Yield 45%;  $R_f = 0.39$  (Ethylacetate/Hexane, 1:20, v/v); mp(Ethylacetate/Hexane): 182–184 °C; IR (KBr)  $\nu_{\max} = 2215$  cm<sup>-1</sup> (CN str.); <sup>1</sup>H NMR (400 MHz, CDCl<sub>3</sub>):  $\delta = 3.10$  (t,  $J = 4.7$  Hz, 4H, 2NCH<sub>2</sub>), 3.49 (t,  $J = 4.7$  Hz, 4H, 2NCH<sub>2</sub>), 3.53–3.62 (m, 4H, Ar-CH<sub>2</sub>-Ar, SCH 2), 4.07 (s, 2H, SCH 2), 6.88–6.93 (m, 1H, Ar–H), 6.97–7.00 (m, 1H, Ar–H), 7.09–7.13 (m, 1H, Ar–H), 7.28–7.30 (m, 1H, Ar–H), 7.38–7.48 (m, 2H, Ar–H), 7.59 (d,  $J = 7.3$  Hz, 1H, Ar–H), 7.90 (d,  $J = 7.6$  Hz, 1H, Ar–H) ppm; <sup>13</sup>C NMR (100.6 MHz, CDCl<sub>3</sub>):  $\delta = 33.8$ , 35.4, 36.7, 52.2, 53.4, 104.9, 114.1, 117.8, 120.1, 121.7, 123.0, 124.6, 126.6, 127.2, 128.0, 131.4, 137.2, 138.9, 139.5, 140.5, 143.7, 145.9, 147.4, 151.4 ppm; MS (ESI) 426 [M + H]<sup>+</sup>; HRMS calculated for C<sub>26</sub>H<sub>24</sub>N<sub>3</sub>OS [M + H]<sup>+</sup> 426.1640, found: 426.1629.

#### 4.2.23. 6-(4-(2-hydroxyphenyl)piperazin-1-yl)-8-(thiophen-2-yl)isothiochromane-5-carbonitrile (**7d**)

Pale yellow solid; Yield 48%;  $R_f = 0.40$  (Ethylacetate/Hexane, 1:20, v/v); mp(Ethylacetate/Hexane): 160–162 °C; IR (KBr)  $\nu_{\max} = 2215$  cm<sup>-1</sup> (CN str.); <sup>1</sup>H NMR (400 MHz, CDCl<sub>3</sub>):  $\delta = 2.96$  (t,  $J = 6.3$  Hz, 2H, Ar-CH<sub>2</sub>), 3.10 (t,  $J = 4.6$  Hz, 4H, 2NCH<sub>2</sub>), 3.29 (t,  $J = 6.4$  Hz, 2H, SCH<sub>2</sub>-CH<sub>2</sub>), 3.37 (t,  $J = 4.6$  Hz, 4H, 2NCH<sub>2</sub>), 3.76 (s,

2H, SCH<sub>2</sub>-Ar), 6.87–6.91 (m, 1H, Ar-H), 6.95–6.97 (m, 1H, Ar-H), 7.00 (s, 1H), 7.05–7.06 (m, 1H, Ar-H), 7.08–7.14 (m, 2H, Ar-H), 7.24–7.26 (m, 2H, Ar-H), 7.43–7.44 (m, 1H, Ar-H) ppm; <sup>13</sup>C NMR (100.6 MHz, CDCl<sub>3</sub>): δ = 25.5, 26.6, 29.7, 52.5, 52.6, 106.7, 114.1, 116.8, 119.2, 120.2, 121.7, 126.7, 126.8, 127.5, 127.8, 129.5, 138.0, 138.5, 140.1, 143.1, 151.3, 154.1 ppm; MS (ESI) 434 [M + H]<sup>+</sup>; HRMS calculated for C<sub>24</sub>H<sub>24</sub>N<sub>3</sub>O<sub>2</sub> [M + H]<sup>+</sup> 434.1361, found: 434.1348.

#### 4.2.24. 6-(4-(2-hydroxyphenyl)piperazin-1-yl)-8-(thiophen-2-yl)isothiochromane-5-carbonitrile (**7e**)

Off white solid; Yield 52%; R<sub>f</sub> = 0.42 (Ethylacetate/Hexane, 1:20, v/v); mp(Ethylacetate/Hexane): 170–172 °C; IR (KBr) ν<sub>max</sub> = 2215 cm<sup>-1</sup> (CN str.); <sup>1</sup>H NMR (400 MHz, CDCl<sub>3</sub>): δ = 2.95 (t, J = 6.4 Hz, 2H, Ar-CH<sub>2</sub>), 3.10 (t, J = 4.3 Hz, 4H, 2NCH<sub>2</sub>), 3.29 (t, J = 6.4 Hz, 2H, SCH<sub>2</sub>-CH<sub>2</sub>), 3.36 (t, J = 4.4 Hz, 4H, 2NCH<sub>2</sub>), 3.54 (s, 2H, SCH<sub>2</sub>-Ar), 6.84 (s, 1H, C<sub>5</sub>-H), 6.87–6.91 (m, 1H, Ar-H), 6.95–6.97 (m, 1H, Ar-H), 7.08–7.12 (m, 1H, Ar-H), 7.17 (d, J = 8.4 Hz, 2H, Ar-H), 7.24–7.26 (m, 2H, Ar-H), 7.60 (d, J = 8.3 Hz, 2H, Ar-H) ppm; <sup>13</sup>C NMR (100.6 MHz, CDCl<sub>3</sub>): δ = 25.5, 26.2, 29.5, 52.6, 52.7, 106.4, 114.1, 116.9, 118.1, 120.2, 121.7, 122.4, 126.7, 128.8, 130.4, 131.8, 138.3, 138.4, 143.3, 144.2, 151.3, 154.3 ppm; MS (ESI) 506 [M + H]<sup>+</sup>, 508 [M + 2 + H]<sup>+</sup>; HRMS calculated for C<sub>26</sub>H<sub>25</sub>BrN<sub>3</sub>OS [M + H]<sup>+</sup> 506.0902, found: 506.0889 and [M + 2 + H]<sup>+</sup> 508.0881, found: 508.0863.

#### 4.3. Cell culture, parasites and infection

J774 cells were maintained in RPMI medium supplemented with fetal bovine serum (Gibco), penicillin (100U/mL) and streptomycin (100 µg/mL) at 37 °C in a humidified (5% CO<sub>2</sub>) atmosphere. *L. donovani* axenic promastigotes (MHOM/IN/80/Dd8) transfected with luciferase gene were maintained in M199 medium supplemented with 10% FBS (Hyclone) and G418 antibiotic (20 µg/mL) at 24 °C. For *in vitro* infection studies, J774 macrophages (4 × 10<sup>4</sup> cells/well) were seeded into 96 well plate and 16 well chamber slide (Thermo Fisher Scientific) for overnight. Macrophages were infected with stationary forms of luciferase transfected Dd8 promastigotes at a 1:8 ratio for 24 h. After infection for 24 h and then treatments with compounds **5a** and **5g**, cells were fixed and stained with Giemsa stain.

#### 4.4. Promastigotes assay

Log phase *L. donovani* promastigotes were seeded in 96-well culture plates with two concentrations (50 µM and 25 µM) of all the compounds dissolved in DMSO. As a vehicle control, promastigotes were only treated with 0.1% DMSO. After 72 post treatment with compounds, cell viability was determined by MTT assay. Briefly, cells were incubated with MTT reagent (20 µL of 5 mg/mL stock in PBS) for 4 h and after incubation cells were transferred to V-shaped bottom 96 well plate. After centrifugation, medium was discarded and 150 µL/well DMSO was added to dissolve the formazan salt. The color intensity of the formazan solution, which reflects the cell growth condition, was measured at 570 nm wavelength using a microplate spectrophotometer (Biotek Powerwave XS2).

#### 4.5. Intracellular amastigotes inhibition assay

Briefly, murine J774 macrophage cell (4 × 10<sup>4</sup>/mL/100 µL/well) were seeded for 24 h in RPMI supplemented with 10% FBS. Cells were then washed and infected with stationary form of luciferase expressing *L. donovani* promastigotes at a ratio of 1:8 (macrophages:parasite) for another 24 h at 37 °C, 5% CO<sub>2</sub>. After incubation, infectivity was checked using Giemsa staining in a parallel set of 16

well chamber slide. Subsequently, non internalized parasites were removed and macrophages with intracellular amastigotes were treated with serial dilution (50 µM–3.125 µM) of the compounds for 72 h. After completion of incubation, cells were observed under microscope and their condition was recorded in a scoring sheet. Furthermore, medium was aspirated from all the wells and equal volume of PBS and steady glo reagent (15 mg/mL) was added to all the wells. To assess the luciferase activity, reading was carried out in a luminometer (Berthold). The IC<sub>50</sub> values of active compounds (**5a**, **5d**, **5e**, **5f**, **5g** and **5h**) were calculated by non-linear regression analysis of dose-response curve using the four-parameter Hill equations. Miltefosine was used as a reference drug for assay.

#### 4.6. Cell cytotoxicity assay using MTT reagent

Cells were seeded to 96 well plates at a starting density of 1 × 10<sup>5</sup> cells/well and cultured overnight. Medium was replaced and macrophages were incubated with graded concentrations of compounds (7.81–500 µM) for another 72 h at 37 °C and 5% CO<sub>2</sub>. Afterwards, 25 µL of MTT (5 mg/mL) was added to cells for 2 h and incubated at 37 °C and 5% CO<sub>2</sub>. Medium was aspirated and resulting formazan was solubilized by adding 150 µL of DMSO to each well. The amount of formazan dye formed was equivalent to the number of live cells and absorbance was read at 570 nm using a microplate spectrophotometer (Biotek Powerwave XS2).

#### 4.7. Detection of phosphatidylserine externalization using flow cytometry

Apoptosis was assessed using flow cytometric analysis of control and **5a** treated promastigotes for different time period that were stained with Alexa fluor 488- Annexin V and PI (Invitrogen). Briefly, log phase promastigotes (1 × 10<sup>6</sup> cells/mL) were seeded into 12 well plate and were treated with **5a** (50 µM) for 24 h, 48 h and 72 h. After incubation, cells were collected, washed in PBS and resuspended in 500 µL of 1X annexin binding buffer. Cells were then incubated with annexin V-Alexa fluor 488 and propidium iodide in the absence of light. After incubation for 15 min, samples were immediately analyzed via BD FACS calibur flow cytometer. Annexin V staining was detected as green fluorescence and PI as red fluorescence.

#### 4.8. Assessment of mitochondrial membrane potential loss

Fluorophore JC-1 was used to study the loss of mitochondrial membrane potential which occurs during cell apoptosis. Briefly, *L. donovani* promastigotes at 1 × 10<sup>6</sup> cells/mL were incubated with 50 µM dose of **5a** for different time period. Promastigotes were incubated with CCCP (50 µM final concentration) as a positive control for induction of depolarization of the mitochondrial membrane potential. At the end of incubation, cells were harvested and washed with PBS. To the cell suspension, 10 µL of 200 µM (2 µM final concentration) JC-1 was added and incubated at 37 °C, 5% CO<sub>2</sub> for 30 min. Afterwards, the cells were washed, resuspended in PBS and analyzed by flow cytometry (FACS calibur).

#### 4.9. TUNEL assay for assessment of DNA fragmentation

DNA fragmentation in *L. donovani* promastigotes treated with **5a** was detected by using APO-BrdU TUNEL Assay Kit (Molecular probes, USA). Briefly, after incubation with **5a** for 72 h, promastigotes were washed with 1X PBS, adhered to poly L-lysine coated slides, and fixed with 4% paraformaldehyde. Next, promastigotes were permeabilized with ice-cold 70% ethanol for 30 min on ice. Slides were then incubated in 50 µL of DNA labeling solution (10 µL

of reaction buffer, 0.75  $\mu$ l of TdT enzyme, 8  $\mu$ l of BrdUTP and 31.25  $\mu$ l of dH<sub>2</sub>O) for 60 min at 37 °C. Cells were stained with 100  $\mu$ l of antibody solution (5  $\mu$ l of Alexa fluor 488 dye labeled anti-BrdU antibody in 95  $\mu$ l of rinse buffer) for 30 min and followed by addition of PI/RNaseA staining buffer for another 30 min. Promastigotes were mounted using Pro-gold anti-fade media (Thermo Fisher Scientific, USA). The broken DNA ends of apoptotic promastigotes were analyzed using confocal microscopy (Zeiss LSM 510 META).

#### 4.10. Ethics Statement

Animal care and experimental procedures were performed in strict accordance by the Committee for the Purpose of Control and Supervision of Experiments on Animals (New Delhi, India). The *in vivo* experimental protocol was approved by the Institutional Animal Ethics Committee (registration no. 34/GO/ReBiBt-S/Re-L/99/CPCSEA) of the Council for Scientific and Industrial Research–Central Drug Research Institute (Lucknow, India) [IAEC approval no: IAEC/2016/101 dated 12.5.16]. For experimental studies, female BALB/c mice (20–25 gm) were housed in climate-controlled and photo period controlled (12-h light/dark cycles) animal house and fed with standard rodent pellets and drinking water ad libitum. Euthanasia of mice was performed by CO<sub>2</sub> inhalation at the end of the experiments.

#### 4.11. Infection and treatment in Balb/c mice

Balb/c mice were divided into five groups, with 5 animals/group. The animals in the group A didn't receive any treatment and termed as infected group. The infected animals in group B received only 5% DMSO as vehicle control. The infected animals in group C received compounds **5a** via intraperitoneal route given for 5 consecutive days at dose of 50 mg/kg. The infected animals in group D received compounds **5g** via intraperitoneal route given for 5 consecutive days at dose of 50 mg/kg. The infected Balb/c mice in group E received miltefosine via oral route as reference drug at a dose of 25 mg/kg daily given for 5 consecutive days. To establish *Leishmania* infection in animals, mice were intravenously infected with stationary phase *Leishmania donovani* promastigotes ( $2 \times 10^7$ ). Infection checking was performed by conducting autopsy of three to four randomly selected mice after 2 wk of infection. For estimation of parasite burden, animals were sacrificed at day 7 post-treatment and tissue samples were obtained from liver and spleen of all groups of Balb/c mice. Afterwards, impression smears were prepared on glass slides, fixed in methanol, stained with 30% Giemsa stain for 2 h. Giemsa stained splenic and liver tissue smear was counted for amastigotes/1000 nucleated cells and was expressed as LDU (1 LDU = amastigote per nucleated cell  $\times$  organ weight in milligram) [24].

#### 4.12. Mitochondria and cytosolic fraction for immunoblot analysis

*L. donovani* promastigotes ( $5 \times 10^7$  cells) were left untreated or treated with **5a** (50  $\mu$ M) for different time periods like 12 h, 24 h, 48 h and 72 h. After incubation, promastigotes were harvested and washed with 1 X PBS, suspended in cell fractionation buffer ApoAlert™ Cell Fractionation Kit (Clontech Laboratories) and incubated on ice for 10 min. Furthermore, cells were homogenized and centrifuged at 10,000 $\times$ g for 25 min at 4 °C to collect the cytosolic fraction and pellet was resuspended in 100  $\mu$ l of Fractionation Buffer Mix to get mitochondrial fraction. Immunoblot analysis was used to detect cytochrome *c* in cytosolic and mitochondrial fractions. Actin and COX-4 were used as loading control for cytosol and mitochondria, respectively.

#### 4.13. Statistical analysis

Data were analyzed using student t-test. The results were expressed as mean values with standard deviations. Statistical significance was considered at  $p < 0.05$  and analysis was performed using Graph Pad Prism version 5.

#### Declaration of competing interest

The authors declare that they have no known competing financial interests or personal relationships that could have appeared to influence the work reported in this paper.

#### Acknowledgment

This study was funded by the Council of Scientific and Industrial Research (CSIR NWP BSC0114), Department of Biotechnology (BT/PR32490/MED/29/1457/2019) New Delhi, India and CSIR-CDRI in house project. AG is thankful to the Department of Atomic Energy (DAE-SRC) for Outstanding Investigator Project Grant (21/13/2015-BRNS/35029). SM, NP, CPS and AS are thankful to University Grants Commission (UGC), New Delhi, Government of India. PC, SP and RPV are thankful to Council of Scientific and Industrial Research (CSIR), New Delhi, Government of India for their financial assistance. The transgenic *L. donovani* promastigotes was a kind gift from Dr. Neena Goyal, Division of Biochemistry, CSIR-CDRI, Lucknow, India. Authors thank SAIF-CDRI, Lucknow, India for providing spectral data, flow cytometry and confocal experiments. This article has CDRI communication number 10238.

#### Appendix A. Supplementary data

Supplementary data to this article can be found online at <https://doi.org/10.1016/j.ejmech.2021.113516>.

#### References

- [1] D. Steverding, The history of leishmaniasis, *Parasites Vectors* 82 (2017) 1–10, <https://doi.org/10.1186/s13071-017-2028-5>.
- [2] F. Frézard, C. Demicheli, R.R. Ribeiro, Pentavalent antimonials: new perspectives for old drugs, *Molecules* 14 (2009) 2317–2336, <https://doi.org/10.3390/molecules14072317>.
- [3] J.A. Lauletta, Review of the current treatments for leishmaniasis, *Res. Rep. Trop. Med.* 3 (2012) 69–77, <https://doi.org/10.2147/RRTM.S24764>.
- [4] H. Sindermann, J. Engel, Development of miltefosine as an oral treatment for leishmaniasis, *Trans. R. Soc. Trop. Med. Hyg.* 100 (Suppl) (2006) S17–S20, <https://doi.org/10.1016/j.trstmh.2006.02.010>.
- [5] G. Gupta, S. Oghumu, A.R. Satoskar, Mechanisms of immune evasion in leishmaniasis, *Adv. Appl. Microbiol.* 82 (2013) 155–184, <https://doi.org/10.1016/B978-0-12-407679-2.00005-3>.
- [6] G.P. McGlacken, I.J.S. Fairlamb, 2-Pyrone natural products and mimetics: isolation, characterisation and biological activity, *Nat. Prod. Rep.* 22 (2005) 369–385, <https://doi.org/10.1039/b416651p>.
- [7] J.M. Dickinson, Microbial pyran-2-ones and dihydropyran-2-ones, *Nat. Prod. Rep.* 10 (1993) 71–98, <https://doi.org/10.1039/np9931000071>.
- [8] I.J.S. Fairlamb, L.R. Marrison, J.M. Dickinson, F.J. Lu, J.P. Schmidt, 2-Pyrones possessing antimicrobial and cytotoxic activities, *Bioorg. Med. Chem.* 12 (2004) 4285–4299, <https://doi.org/10.1016/j.bmc.2004.01.051>.
- [9] V.J. Ram, A. Goel, P.K. Shukla, A. Kapil, Synthesis of thiophenes and thieno[3,2-*c*]pyran-4-ones as antileishmanial and antifungal agents, *Bioorg. Med. Chem. Lett.* 7 (1997) 3101–3106, [https://doi.org/10.1016/S0960-894X\(97\)10153-6](https://doi.org/10.1016/S0960-894X(97)10153-6).
- [10] A.G. Tempone, D.D. Ferreira, M.L. Lima, T.A. Costa Silva, S.E.T. Borborema, J.Q. Reimão, M.K. Galuppo, J.M. Guerra, A.J. Russell, G.M. Wynne, R.Y.L. Lai, M.M. Cadelis, B.R. Copp, Efficacy of a series of alpha-pyrone derivatives against *Leishmania* (L.) infantum and *Trypanosoma cruzi*, *Eur. J. Med. Chem.* 139 (2017) 947–960, <https://doi.org/10.1016/j.ejmech.2017.08.055>.
- [11] O. Kayser, A.F. Kiderlen, S.L. Croft, Antileishmanial activity of two  $\gamma$ -pyrones from *Podolepis hieracioides* (Asteraceae), *Acta Trop.* 86 (2003) 105–107, [https://doi.org/10.1016/S0001-706X\(02\)00258-9](https://doi.org/10.1016/S0001-706X(02)00258-9).
- [12] N. Chandra, Ashutosh Ramesh, N. Goyal, S.N. Suryawanshi, S. Gupta, Antileishmanial agents part-IV: synthesis and antileishmanial activity of novel terpenyl pyrimidines, *Eur. J. Med. Chem.* 40 (2005) 552–556, <https://doi.org/10.1016/j.ejmech.2005.01.004>.

- [13] A. Mayence, J.J. Vanden Eynde, L. LeCour, L.A. Walker, B.L. Tekwani, T.L. Huang, Piperazine-linked bisbenzamidines: a novel class of antileishmanial agents, *Eur. J. Med. Chem.* 39 (2004) 547–553, <https://doi.org/10.1016/j.ejmech.2004.01.009>.
- [14] F. Poorrajab, S.K. Ardestani, S. Emami, M. Behrouzi-Fardmoghdam, A. Shafiee, A. Foroumadi, Nitroimidazolyl-1,3,4-thiadiazole-based anti-leishmanial agents: synthesis and in vitro biological evaluation, *Eur. J. Med. Chem.* 44 (2009) 1758–1762, <https://doi.org/10.1016/j.ejmech.2008.03.039>.
- [15] C.E. Mowbray, S. Braillard, W. Speed, P.A. Glossop, G.A. Whitlock, K.R. Gibson, J.E.J. Mills, A.D. Brown, J.M.F. Gardner, Y. Cao, W. Hua, G.L. Morgans, P.B. Feijens, A. Matheussen, L.J. Maes, Novel amino-pyrazole ureas with potent in vitro and in vivo antileishmanial activity, *J. Med. Chem.* 58 (2015) 9615–9624, <https://doi.org/10.1021/acs.jmedchem.5b01456>.
- [16] H.T. Takahashi, C.R. Novello, T. Ueda-Nakamura, B.P.D. Filho, J.C.P. De Mello, C.V. Nakamura, Thiophene derivatives with antileishmanial activity isolated from aerial parts of *Porophyllum ruderale* (Jacq.) Cass, *Molecules* 16 (2011) 3469–3478, <https://doi.org/10.3390/molecules16053469>.
- [17] A. Goel, V.J. Ram, Natural and synthetic 2H-pyran-2-ones and their versatility in organic synthesis, *Tetrahedron* 65 (2009) 7865–7913, <https://doi.org/10.1002/CHIN.200950230>.
- [18] <http://www.molinspiration.com>. (Accessed August 2020).
- [19] C.A. Lipinski, F. Lombardo, B.W. Dominy, P.J. Feeney, Experimental and computational approaches to estimate solubility and permeability in drug discovery and development settings, *Adv. Drug Deliv. Rev.* 23 (1997) 3–25, [https://doi.org/10.1016/S0169-409X\(00\)00129-0](https://doi.org/10.1016/S0169-409X(00)00129-0).
- [20] D.F. Veber, S.R. Johnson, H.Y. Cheng, B.R. Smith, K.W. Ward, K.D. Kopple, Molecular properties that influence the oral bioavailability of drug candidates, *J. Med. Chem.* 12 (2002) 2615–2623, <https://doi.org/10.1021/jm020017n>.
- [21] P. Ertl, B. Rohde, P. Selzer, Fast calculation of molecular polar surface area as a sum of fragment-based contributions and its application to the prediction of drug transport properties, *J. Med. Chem.* 43 (2000) 3714–3717, <https://doi.org/10.1021/jm000942e>.
- [22] T. Sander, Idorsia Pharmaceuticals Ltd, Hegenheimermattweg 91, 4123 Allschwil, Switzerland, <https://www.organic-chemistry.org/prog/peo/>.
- [23] S. Gannavaram, A. Debrabant, S.M. Beverley, Programmed Cell Death in Leishmania : Biochemical Evidence and Role in Parasite Infectivity, vol. 2, 2012, pp. 1–9, <https://doi.org/10.3389/fcimb.2012.0009>.
- [24] A. Upadhyay, P. Chandrakar, S. Gupta, N. Parmar, S.K. Singh, M. Rashid, P. Kushwaha, M. Wahajuddin, K.V. Sashidhara, S. Kar, Synthesis, biological evaluation, structure–activity relationship, and mechanism of action studies of quinoline-metronidazole derivatives against experimental visceral leishmaniasis, *J. Med. Chem.* 62 (2019) 5655–5671, <https://doi.org/10.1021/acs.jmedchem.9b00628>.